Image Cover Sheet

CLASSIFICATION	SYSTEM NUMBER
UNCLASSIFIED	517628

TITLE

Modulation recognition algorithms for Intentional Modulation on Pulse \(IMOP\) applications

System Number:

Patron Number:

Requester:

Notes:

DSIS Use only:

Deliver to: DK

This page is left blank

This page is left blank

DEFENCE R&D DÉFENSE

Modulation Recognition Algorithms for Intentional Modulation on Pulse (IMOP) Applications

Stephen Sung and Yifeng Zhou

Defence R&D Canada
TECHNICAL REPORT
DREO TR 2001-111
December 2001

National Defence Défense nationale

Canada

Modulation Recognition Algorithms for Intentional Modulation on Pulse (IMOP) Applications

Stephen Sung
Intrinsix Canada Company

Yifeng Zhou
DREO

Defence Research Establishment Ottawa

Technical Report

DREO TR 2001-111

December 2001

Author

Yifeng Zhou

Approved by

Pierre Yansouni
Head/Electronic Support Measures Section

Approved for release by

Gordon Marwood
Chair/Document Review Panel

Abstract

In this report, the problem of signal modulation classification is investigated. A modulation recognition algorithm for classifying different signal modulation types and noise is described. The modulation type includes unmodulated CW, narrow-band FM, wide-band FM, triangular FM, BPSK, DSB-SC and AM. The algorithm involves a combination of decision theoretic and pattern recognition techniques. The decision theoretic technique is based on the calculation of a number of statistics of the input sequence to be classified. It is used to separate noise from the signals, the constant-envelope waveforms from the varying-envelope waveforms, the unmodulated CW from the waveforms with phase information, and the two varying-envelope waveforms from one another The pattern recognition technique is used to distinguish the three FM and BPSK waveforms The technique is based on the use of a linear discriminant. The discriminant is trained by feature vectors generated from the residual-phase histogram. Finally, computer simulations are used to demonstrate the performance of the proposed modulation recognition algorithm, and an extensive analysis is also included.

Résumé

Dans ce rapport, le problème de la classification de modulation des signaux est étudié Un algorithme d'identification de modulation pour classifier les différents types de modulation de signaux et de bruit est décrit. Les types de modulations comprennent les signaux non modulé CW, FM à bande étroite, FM à large bande, FM triangulaire, BPSK, DSB-SC et AM. L'algorithme comporte une combinaison de techniques théorique de décision et de reconnaissance des formes La technique théorique de décision est basée sur le calcul d'un certain nombre de statistiques de la sequence d'entrée à classifier. Elle est employée pour séparer le bruit des signaux, les formes d'onde d'enveloppe constante des formes d'onde avec enveloppe variable, les signaux non modulé CW des formes d'onde avec information dans la phase, et pour séparer deux formes d'onde avec enveloppe variable La technique de reconnaissance des formes est employée pour distinguer les trois formes d'onde FM et la forme d'onde BPSK. La technique est basée sur l'utilisation d'un discriminant linéaire Le discriminant est formé de vecteurs d'attributs produits par l'histogramme de la phase residuel. En conclusion, des simulations par ordinateur sont employées pour démontrer la performance de l'algorithme d'identification de modulation proposé, et une analyse généralisée est également incluse

This page intentionally left blank.

Executive summary

Recently, there has been increasing interest in developing techniques that exploit the intrapulse information of emitter signals. Intrapulse information refers to the shape of the pulse envelope and waveform modulation of a signal. It carries rich information about the emitter system characteristics and can be used to classify emitter systems. In this report, we investigate the radar signal modulation classification problems. Radar signal modulation classification is important for ESM and ELINT applications for three reasons. Firstly, the modulation type of a signal itself is an important intrapulse parameter for recognizing the radar type. Secondly, knowing the correct signal modulation type is critical to determining other intrapulse parameters such as the carrier frequency. Thirdly, it can also help the radar warning system to distinguish between a communications signal and a radar signal.

In this report, a modulation recognition algorithm for classifying radar signal modulation types and noise is proposed. The modulation type includes unmodulated CW, narrow-band FM, wide-band FM, triangular FM, BPSK, DSB-SC and AM. The algorithm involves a combination of decision theoretic and pattern recognition techniques. The decision theoretic technique is based on the calculation of a number of statistics of the sample sequence to be classified. It is used to separate noise from the signals, the constant-envelope waveforms from the varying-envelope waveforms, the unmodulated CW from the waveforms with phase information, and the two varying-envelope waveforms from one another. The pattern recognition technique is used to distinguish the three FM and BPSK waveforms. It uses the residual-phase histogram as the feature vector and a linear discriminant. The linear discriminant is trained using simulated signals with different modulation types and varying parameters. Our investigation of the use of residual-phase and instantaneous-frequency histograms as feature vectors is reported. There seems to be sufficient differentiation among the residual-phase histograms of the four waveforms to justify the use of these histograms alone, without the instantaneous-frequency histograms, as feature vectors. It is found that phase histograms consisting of 20 bins over the interval work well. After the modulation type is determined, the waveform parameters are estimated for most of the waveforms, including the FM and AM modulation frequencies, the carrier frequencies, the signal amplitude, the FM peak frequency deviation and the AM modulation index.

The performance of the proposed decision tree is demonstrated using computer simulated data. A sample sequence is generated for different combination of varied parameter values. The number of sequences so generated ranges from 90 to 250, depending on the waveform. A sampling frequency of $1.8MS/s$ and a sample size of 1024 are considered to be suitable for the set of radar signals under consideration. Accordingly, these values are used in our simulation studies.

Stephen Sung and Yifeng Zhou. 2002. Modulation Recognition Algorithms for Intentional Modulation on Pulse (IMOP) Applications. DREO TR 2001-111. Defence Research Establishment Ottawa.

Sommaire

Récemment, l'intérêt du développement de techniques pour exploiter l'information d'intrapulse de signaux augmente. L'information d'intrapulse se rapporte à la forme de l'enveloppe d'impulsion et à la modulation de forme d'onde d'un signal. Elle porte de l'information sur les caractéristiques du système d'émetteur et peut être utilisée pour les classifiers. Dans ce rapport, nous étudions les problèmes de classification de modulation de signal de radar. La classification de modulation de signal de radar est importante en demandes d'ESM et d'ELINT pour trois raisons. Premièrement, le type de modulation d'un signal est un paramtre d'intrapulse important pour identifier le type de radar. Deuxièmement, la modulation du signal est critique pour déterminer autres paramètres d'intrapulse tels que la fréquence porteuse Troisièmement, elle peut également aider le système d'alerte radar à distinguer un signal de transmissions et un signal de radar.

Dans ce document, un algorithme d'identification de modulation pour classifier des types de modulation de signal de radar et de bruit est proposé. Les types de modulations comprennent les signaux non modulé CW, FM à bande é'troite, FM à large bande, FM triangulaire, BPSK, DSB-SC et AM. L'algorithme comporte une combinaison de techniques théorique de décision et de reconnaissance de formes La technique théorique de décision est basée sur le calcul d'un certain nombre de statistiques de la sequence d'entrée que l'on désire classifier Elle est employée pour séparer le bruit des signaux, les formes d'onde d'enveloppe constante des formes d'onde avec enveloppe variable, les signaux non modulé CW des formes d'onde avec information dans la phase, et pour séparer deux formes d'onde avec enveloppe variable La technique de reconnaissance des formes est employée pour distinguer les trois formes d'onde FM et la forme d'onde BPSK La technique est basée sur l'utilisation d'un discriminant linéaire formé de vecteurs d'attributs produits par l'histogramme de la phase residuel Le discriminant linéaire est formé en utilisant des signaux simulés avec différents types de modulation et avec des parametres variables Notre recherche sur l'utilisation d'histogrammes de la phase residuel avec et d'histogrammes de la fréquence instantanée comme vecteurs d'attributs est dans le rapport. Il semble y avoir assez de différences parmi les histogrammes de la phase residuel des quatre formes d'onde pour justifier l'utilisation de ces histogrammes, sans les histogrammes de la fréquence instantanée, comme vecteurs d'attributs On trouve que les histogrammes de phase se composant de 20 emplacements, au travers l'intervalle de travail, fonction bien Après avoir déterminé le type de modulation, les paramètres de forme d'onde sont estimés pour la plupart des formes d'onde, y compris les fréquences de modulation FM et AM, les fréquences porteuses, l'amplitude de signaux, la déviation maximale en fréquence de modulation FM et l'indice de modulation AM

La performance de l'arbre de décision proposé est démontrée en utilisant des données simulées par ordinateur Une séquence d'échantillon est produite pour différente combinaison de valeur des paramètres. Le nombre de séquences produites s'étend de 90 à 250, selon la forme d'onde. Une fréquence d'echantillonnage de 1.8MS/s et une

dimension d'échantillon de 1024 sont considérées appropriées à l'ensemble de signaux de radar à l'étude. En conséquence, ces valeurs sont utilises dans les simulations étudiées.

Stephen Sung and Yifeng Zhou. 2002. Modulation Recognition Algorithms for Intentional Modulation on Pulse (IMOP) Applications DREO TR 2001-111. Centre de recherches pour la défense, Ottawa.

Table of contents

List of figures

List of tables

This page intentionally left blank

1. Introduction

In Electronic Support Measures (ESM) and Electronic Intelligence (ELINT) systems, receivers are designed to intercept transmitted signals and perform emitter classification and identification for electronic warfare (EW) purposes. Conventional systems characterize the signals based on the use of coarse conventional parameters such as direction-of-arrival (DOA), radio frequency (RF), time-of-arrival (TOA), pulse width (PW), pulse repetition interval (PRI) and polarization. They encounter difficulties with the proliferation of radar signals and modern radars employing sophisticated digital processing systems. Recently, there has been increasing interest in developing techniques which exploit the intrapulse information of emitter signals. Intrapulse information refers to the shape of the pulse envelope and waveform modulation of a signal. It carries rich information about the emitter system characteristics and can be used to classify emitter systems. In this report, we investigate the radar signal modulation classification problem. Radar signal modulation classification is important for ESM and ELINT applications for three reasons. Firstly, the modulation type of a signal itself is an important intrapulse parameter for recognizing the radar type. Secondly, knowing the correct signal modulation type is critical to determining other intrapulse parameters such as the carrier frequency. Thirdly, it can also help the radar warning system to distinguish between a communications signal and a radar signal.

In order to obtain information on communication signals, we studied the Technical and Administrative Frequency List (TAFL), a database of nation-wide transmitters and receivers for which licenses have been granted. The TAFL database can be accessed through http://spectrum.ic.gc.ca/tafl/tafindxe.html. Each entry of the database contains such useful information as transmit and/or receive frequency, bandwidth, spectrum signature (e.g., 600 frequency-division-multiplexed, frequency-modulated voice channels), and antenna pattern data. A detailed list of the technical information available from the database is given in Annex A. The database has been organized in two ways: according to five regions across Canada (Pacific, Central, Ontario, Quebec and Atlantic) and by frequency ranges. Each geographical region is divided into smaller regions. The Ontario region, for example, is divided into sub-regions covering eastern Ontario, northern Ontario, central and western Ontario, Toronto, Hamilton, etc. Similarly, each frequency range is divided into a number of frequency bands.

The definition of the communication-signal environment along a flight path using the TAFL database is a major undertaking. All the transmitters within the reception range of the warning receiver must be retrieved from the database. In addition to parameters such as transmit frequency and bandwidth that are clearly important, antenna parameters such as beam-pointing direction and azimuthal beamwidth are also important in determining the time when the plane first enters a beam and the time it spends within the beam. In view of the complexity of the communication-signal environment, little effort was made to model communication signals in this study. Instead, a cursory examination of the TAFL database was made to obtain some idea of the bandwidths involved. In many cases, the transmission bandwidth is of the order of

several tens of megahertz By comparison, the largest bandwidth of the radar signals studied is several megahertz. This confirms the oft-held view that communication bandwidths are often much larger than radar bandwidths

For the sampling frequency and sample size considered in this study, the waveforms amount to the following eight: (1) unmodulated CW, (2) amplitude modulated (AM), (3) double sideband, suppressed carrier (DSB-SC), (4) narrow-band frequency modulated (FM), (5) wide-band FM, (6) triangular FM, (7) binary phase shift keyed (BPSK), and (8) noise In waveform (6), the instantaneous frequency consists of an up-slope and a down-slope, of equal magnitude and symmetrically placed within the observation duration In waveform (7), the phase shift on a state change is 90°, 120° or 155° rather than 180°

A modulation classification algorithm is proposed based on the application of two approaches· the decision theoretic approach [1]-[5] and the pattern recognition approach [1][6]-[8] In the decision theoretic approach, a statistic based on an appropriate quantity is calculated from the sample sequence and compared with a threshold. If the value of the statistic, referred to as a feature, is less than the threshold, then the sample sequence is put in one class; otherwise, the sample sequence is put in another class A decision tree is then devised, involving the calculation of a relatively small number (e.g., several) of features and the comparison with their thresholds. The processing of a test sequence (i.e , a sequence of unknown modulation) by the decision tree results in the sequence being placed in one of several modulation classes A drawback of this approach is that it is not always possible to find a set of features that would allow all the modulations of interest to be distinguished. In the pattern recognition approach, a feature vector is extracted from a sample sequence The dimensionality of this feature vector can be, e g , several tens An example of a feature vector is one where the components are the populations of a phase histogram A training data set, consisting of feature vectors from all the modulation classes of interest, is first generated A pattern classification algorithm and its associated decision rule are then chosen and trained using the feature vectors from the training data set to arrive at an actual implementation of the algorithm This implementation allows the modulation type of a test sequence to be determined. The pattern classification algorithm can be evaluated by generating a validation data set, similar to the training data set, and letting the algorithm operate on each feature vector of the set. The resulting confusion matrix gives an indication of how good the pattern classification algorithm and its training are

In the hybrid decision tree, the decision theoretic approach is used to separate noise from signals, constant-envelope waveforms from DSB-SC and AM, unmodulated CW from the three FMs and BPSK, and DSB-SC from AM, while the pattern recognition approach is used to distinguish the three FMs and BPSK In the algorithm, the power spectral density (PSD) is first estimated The noise threshold is derived and used to decide if a sequence contains noise samples only. Noise testing can be implemented both in the time and in the frequency domain Once the signal is detected, the centroid

frequency is estimated as the first estimate of the carrier frequency and the waveform is demodulated by this estimate. The waveform envelope and the unwrapped residual phase are calculated. A straight line is fit to the unwrapped residual phase, and the detrended residual phase is obtained. A statistic based on the square of the waveform envelope is used to separate the constant-envelope waveforms from DSB-SC/AM and DSB-SC from AM. The mean square of the detrended residual phase is used as the statistic to determine the absence or presence of phase information, and thus to separate unmodulated CW from the three FMs and BPSK. The pattern classification approach involves linear discriminants [7][8]. The coefficients of a linear discriminant are obtained by minimizing the sum of the squares of the errors of classifying all the normalized feature vectors of the training data set The detrended residual-phase histogram of the three FM and BPSK waveforms is input into the trained linear discriminant, and the decision rule gives the modulation type.

For most of the waveforms, after the modulation type is determined, the waveform parameters are estimated. The estimation accuracy depends on the parameter. Parameters such as the FM and AM modulation frequencies are estimated using the method developed by Crozier and collaborators [9][10]. Parameters such as the signal amplitude, the FM peak frequency deviation and the AM modulation index, however, are estimated only crudely. These latter parameters are estimated by simply examining how they can be obtained if noise could be neglected The assumption that a sample sequence spans an integral number of modulation cycles is also made To study the recognition of the eight waveforms, a sampling frequency of $1.8MS/s$ and a sample size of 1024 are considered to be suitable for the set of radar signals under consideration. Accordingly, these values are used in our simulation studies.

The report is organized as follows. The signal and noise model is formulated in Section 2. In Section 3, the decision theoretic approach is discussed The pattern recognition approach of the decision tree is discussed in Section 4. Our investigation of the use of detrended residual-phase and instantaneous-frequency histograms as feature vectors is reported. In Section 5, the proposed modulation recognition algorithm is discussed and detailed implementation issues are provided Also in this section, the performance of the proposed decision tree is demonstrated using computer simulated data. Finally, a conclusive summary is given in Section 6

2. Signal and Noise Modeling

Consider the following eight signal types of interest: (1) unmodulated CW, (2) amplitude modulated (AM), (3) double sideband, suppressed carrier (DSB-SC), (4) narrow-band frequency modulated (FM), (5) wide-band FM, (6) triangular FM, (7) binary phase shift keyed (BPSK), and (8) noise They can be described as follows.

(1)Unmodulated:

$$s(n) = A\exp[j(\phi + 2\pi f_c Tn)], \quad n = 1, 2, \ldots, N, \tag{1}$$

where A denotes the carrier amplitude, ϕ an unknown phase, f_c the carrier frequency, T the sampling interval and N the number of samples

(2)AM·

$$s(n) = A[1 + m\cos 2\pi f_{am} Tn]\exp[j(\phi + 2\pi f_c Tn)], \quad n = 1, 2, \ldots, N, \tag{2}$$

where m is the modulation index and f_{am} is the frequency of the message signal

(3)DSB-SC.

$$s(n) = A\cos 2\pi f_{am} Tn\exp[j(\phi + 2\pi f_c Tn)], \quad n = 1, 2, \ldots, N. \tag{3}$$

(4)Narrow-band FM·

$$s(n) = A\exp[j(\phi + 2\pi f_c Tn + \frac{\Delta f}{2f_m}\sin 2\pi f_m Tn)], \quad n = 1, 2, \ldots, N, \tag{4}$$

where $\Delta f/2$ is the peak deviation and f_m is the frequency of the sinusoidal frequency modulation By narrow-band FM, we mean that $\Delta f/2f_m \gg 1$. It is also assumed that many cycles of the modulation are sampled over the observation duration

(5)Wide-band FM

The wide-band FM signal model is described by (4) The wide-band FM signal is characterized by $\Delta f/2f_m \gg 1$, and only a fraction of a cycle of the modulation is sampled over the observation duration.

(6)Triangular FM

$$s(n) = \begin{cases} \exp[j(\phi + 2\pi f_c Tn + \pi\alpha T^2 n^2)] & n = -N/2, -N/2+1, \ldots, -1 \\ \exp[j(\phi + 2\pi f_c Tn - \pi\alpha T^2 n^2)] & n = 0, 1, \ldots, N/2-1 \end{cases} \tag{5}$$

where α is the slope of the instantaneous-frequency up-ramp. The slope of the down-ramp has the same magnitude The up- and down-ramps are symmetric within

the observation duration The frequency f_c is the instantaneous frequency at the apex of the triangular frequency variation, which is the maximum instantaneous frequency within the observation duration. The slope α is calculated as $2\Delta/\tau$, where Δ is the bandwidth within the time period τ The parameter τ is a fixed value. The waveform is considered to be characterized by f_c and Δ rather than by f_c and α.

(7)BPSK

$$s(n) = A\exp[j(\phi + 2\pi f_c T n + \theta(n))], \quad n = 1, 2, \ldots, N, \tag{6}$$

where $\theta_n = 0$ when the zero bits of the code sequence are sampled and $\theta_n = \theta$ when the one bits of the code sequence are sampled. The phase shift θ can be 90^o, 120^o or 155^o The code sequence consists of 15 bits and is repeated every $1/f_{psk}$ second The frequency f_{psk} is such that many cycles of the code sequence are sampled within the observation duration.

(8)Noise

The noise samples $w(n)$ are modeled as additive, white, complex Gaussian process with zero mean and variance $2\sigma^2$

In practice, the received signal is always corrupted by noise which includes medium ambient noise, antenna thermal noise, the circuitry noise, *etc.*. The noise can be described by the above Gaussian noise model. Let $z(n)$ denote the noisy signal samples Then, we have

$$z(n) = s(n) + w(n), \quad n = 1, 2, \ldots, N, \tag{7}$$

where $s(n)$ can be one of the seven signals mentioned above when the signal is present or a null signal in the absence of any signals. Also note that many receivers down-convert (e g , an IMOP receiver) the carrier frequency to an intermediate frequency (IF) prior to processing Thus, in equations (1) to (6), f_c is really an IF rather than a carrier frequency In the simulation studies, the IF is chosen to vary from $100kHz$ to $800kHz$

3. Decision Theoretic Approach

The decision theoretic approach is based on certain statistics of the the sample sequence for discrimination between the modulation types of interest. The statistic calculated from the sample sequence is referred to as a feature. Based on the value of the statistic, the sample sequence is put in appropriate class. A decision tree is then devised, involving the calculation of a relatively small number (e.g., several) of features and the comparison with their thresholds The processing of an input sequence with unknown

modulation type by the decision tree results in the sequence being placed in one of several modulation classes In our proposed decision theoretic approach, the sample sequence is separated in the following steps: (1) noise from the seven signals; (2) the constant-envelope waveforms (unmodulated CW, the three FMs and BPSK) from the varying-envelope waveforms (DSB-SC and AM); (3) the signal with no phase information (unmodulated CW) from the signals with phase information (the three FMs and BPSK); and (4) DSB-SC from AM. Each of these separations involves a comparison with a preset threshold The selection of the values of these thresholds would have critical impact on the final separation performance

In separating the signals, the power spectral density (PSD) is first calculated from the input sequence. There are different techniques for estimating the PSDs including the ones based on periodogram averaging such as Welch's method [11] A sample sequence was simulated to a length of 8192, which was then divided into 15, 1024-point, 50%-overlapping sections. Each section was Hanning windowed and discrete Fourier transformed (DFTed). The magnitude squared of the DFT components were then averaged over the sections In general, the periodogram averaging approach performs well for stationary signals It may not be suitable for nonstationary signals such as the triangular FM signal. In our simulation study, the PSD is generated instead by simulating the input sequence to a length of only 1024 and then calculating the magnitude squared of the DFT of this sequence

3.1 Noise Threshold

The test to determine if a sample sequence is noise only or contains a signal can be carried out either in the time domain or in the frequency domain Consider the time domain approach. Since $w(n)$ is assumed to be a complex Gaussian process with zero mean and variance $2\sigma^2$, it can be verified that its power, $P_w(n) = \mid w(n) \mid^2$, is exponentially distributed, with a probability density function (pdf) given by

$$p\{P_w(n)\} = \frac{1}{2\sigma^2} \exp\{-\frac{P_w(n)}{2\sigma^2}\}, \tag{8}$$

The time domain approach is to compare the magnitude squared of each sequence sample with the threshold, $P_{T,time}$ The sequence is considered as noise only if the number of samples exceeding the threshold is smaller than or equal to a certain number K One may require K to be zero, i e , none of the sample powers should exceed the threshold in order for the sequence to qualify as noise only This requirement, however, may be too stringent, since if a sufficiently large number of noise sequences are considered, there will be samples with powers that exceed the threshold Thus, for example, if 10,000 sequences of 1024 samples each are considered and a false alarm probability of $P_{fa} = 10^{-6}$ is required, we would expect that about 10 samples would have powers exceeding the threshold A sequence with, say, one sample exceeding the threshold can be a genuine noise sequence. Hence, K is set to one in our study, a value that seems to work well in actual testing.

Given a threshold $P_{T,time}$, the probability of false alarm can be obtained as

$$P_{fa} = \int_{P_{T,time}}^{\infty} p\{P_w(n)\} dP_w(n) = \exp\{-\frac{P_{T,time}}{2\sigma^2}\}, \tag{9}$$

Form (9), we can obtain the relationship between the threshold and the resulting false alarm as $P_{T,time} = -2\sigma^2 \ln P_{fa}$.

The frequency domain approach is based on the statistics of the DFT components of a noise sequence. Using the fact that the noise samples have the properties

$$E[w(j)] = 0, \quad E[w(j)w(k)] = 0 \text{ and } E[w(j)w^*(k)] = 2\sigma^2\delta_{jk}, \tag{10}$$

where $E[\cdot]$ denotes the expectation operation, $*$ complex conjugation and δ_{jk} is the Kronecker delta, it follows that the DFT components

$$W(m) = \sum_{n=0}^{N-1} w(n) \exp\{-j2\pi mn\}, \quad m = 0, 1, \quad ..N-1, \tag{11}$$

is zero mean and

$$E[W(j)W(k)] = 0 \text{ and } E[W(j)W^*(k)] = 2N\sigma^2\delta_{jk}. \tag{12}$$

Since $W(m)$ is a linear combination of normal random variables, they are normal random variables. Properties in (12) imply that the DFT of an $i.i.d$ zero mean circular complex Gaussian process with variance $2\sigma^2$ is an $i.i.d$ zero mean circular complex Gaussian with variance $2N\sigma^2$. It follows that $\mid W(m) \mid^2$ is exponentially distributed with an average value of $2N\sigma^2$. Let $P_{T,freq}$ denote the threshold in the frequency domain. By using the same argument as that in the time domain approach, it can be obtained that

$$P_{T,freq} = -2N\sigma^2 \ln P_{fa} = NP_{T,time}. \tag{13}$$

The criterion for determining a noise sequence is that no more than one value of $\mid W(m) \mid^2$ should exceed $P_{T,freq}$. It will be seen later that since the PSD of a sample sequence would be required for the carrier frequency estimation, the frequency domain approach does not cost any extra computations in terms of the complete modulation recognition algorithm.

3.2 Centroid Frequency Calculation

When the sample sequence is determined as containing a signal, the next step is to estimate it centroid frequency We only use those effective samples for frequency estimation By effective samples, we mean those samples with amplitude above a certain threshold It is known that several modulation types are likely to be affected by the noise in the weak interval of a signal. Thus, it is not advantageous to use those heavily noise contaminated samples. The effective samples are selected as follows First, the maximum value of the PSD is determined. Then, a threshold equal to one-third of this maximum value is used to delimit the PSD samples involved in the calculation of the centroid frequency. Let n_1, and n_2 denote the index of the first and the last sample, respectively, of the PSD that exceed the threshold. Denoting the PSD samples by $S(n)$ and the frequency values by $F(n) = nf_s/N$, the centroid frequency is computed as the PSD-weighted average by

$$\hat{f}_{c,1} = \frac{\sum_{n_1}^{n_2} S(n)F(n)}{\sum_{n_1}^{n_2} S(n)}. \tag{14}$$

Note that $\hat{f}_{c,1}$ is a coarse estimate of f_c and is used to demodulate the sequence samples. The demodulated sequence $\tilde{z}(n)$ is given by

$$\tilde{z}(n) = z(n) \exp\{-\jmath 2\pi \hat{f}_{c,1} T n\}. \tag{15}$$

3.3 Square-of-envelope Statistic

The separation of the constant-envelope waveforms from DSB-SC and AM and the latter two from each other is based on the square-of-envelope statistic defined by

$$R = \frac{< E^4(n) > - < E^2(n) >^2}{< E^2(n) >^2}, \tag{16}$$

where $E(n)$ denotes the amplitude and the angle brackets denote averages over samples This ratio is the variance of the square of the envelope normalized by the square of its mean The use of this statistic to separate waveforms has been investigated by Chan and Gadbois [5] We have carried out a study of the dependence of R on the carrier-to-noise ratio (CNR) for each of these three waveforms: unmodulated CW, DSB-SC and AM For DSB-SC, the CNR is interpreted as the signal-to-noise ratio (SNR) The results are summarized in Figure 1. For each of the three waveforms and at each CNR, 1000 sample sequences are generated to obtain the averaged ratio R. It is seen that constant-envelope waveforms can be readily separated from DSB-SC and AM For example at the minimum CNR, 15dB, a threshold of 0.08 can be set on R, below which the waveform is classified as constant-envelope The separation of AM

from DSB-SC is less clear-cut because the R curve for AM depends on the modulation index. In the limit of infinite CNR, it is simple to show that R for AM, R_{AM}, depends on the modulation index, m, as

$$R_{AM} = \frac{2m^2(1 + m^2/16)}{(1 + m^2/2)^2}. \tag{17}$$

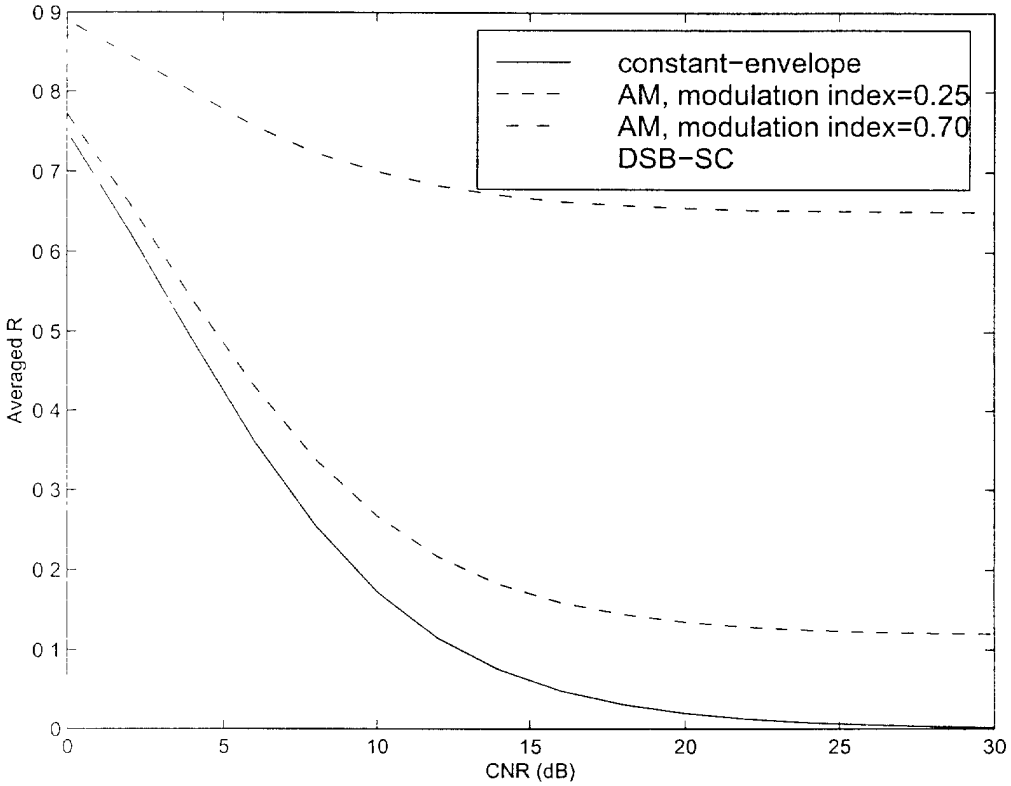

Figure 1 Variation of R versus CNR for constant-envelope, AM and DSB-SC modulations

A plot of R_{AM} versus m is shown in Figure 2. For $m = 0.25$ and 0.7, R_{AM} is 0.118 and 0.652, respectively. From Figure 1, it is seen that the two AM curves approach these values at high CNRs. For DSB-SC, R in the limit of infinite CNR is equal to 0.5, which is also borne out by the DSB-SC curve in Figure 1. If the AM modulation index is in the neighborhood of 0.6, so that R_{AM} is in neighborhood of 0.5, the AM and the DSB-SC curves would be close together, and it would not be possible to separate these two waveforms on the basis of their R values. Such an AM modulation index, however, does not seem to arise in most radars of interest. As well, a modulation index of 0.25 seems to be the minimum for these radars. A band of R values, $0.47 < R < 0.56$, is therefore used to discriminate between a DSB-SC and an AM modulation type.

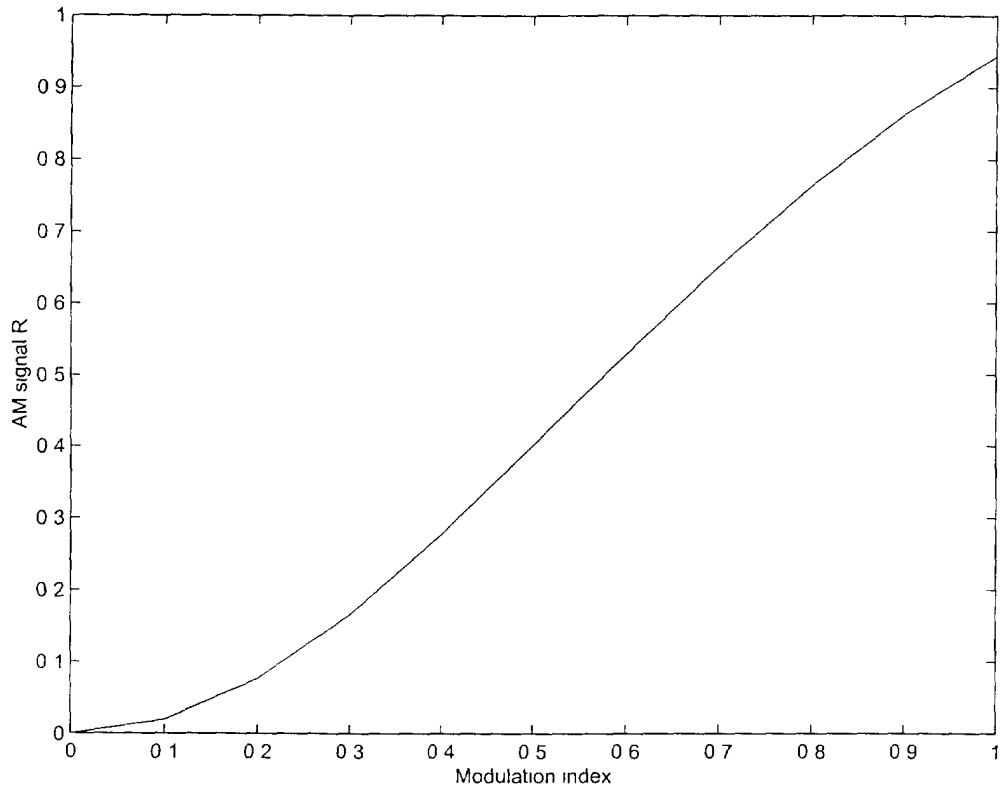

Figure 2: *The square-of-envelope statistic for sinusoidal AM as a function of the modulation index*

3.4 Detrended Residual Phase Statistic

Phase unwrapping is an important step, since any trend in the residual phase would not be apparent unless its values are first unwrapped. This is illustrated for the narrow-band FM and BPSK modulations in the two plots in the top row of Figure 3 In each plot, the dotted curve is the residual phase restricted to the interval $(-\pi, \pi)$, and the solid curve is the unwrapped residual phase. The linear trend is clear only after phase unwrapping. A least-squares straight line is fit to the unwrapped residual phase and then subtracted from it to give the detrended residual phase $\delta\phi(n)$, shown in the plots in the bottom row of Figure 3 Only the first 400 samples of each sequence are plotted to show the oscillatory nature of the narrow-band FM detrended residual phase and the repetitive nature of the BPSK detrended residual phase.

The linear trend is a reflection of the fact that $\hat{f}_{c,1}$ is not exactly equal to f_c and therefore the unwrapped residual phase contains the linear term $2\pi(f_c - \hat{f}_{c,1})Tn$. By fitting a least-squares straight line to the unwrapped residual phase, the slope of the straight line gives an estimate of $f_c - \hat{f}_{c,1}$, which is then added to $\hat{f}_{c,1}$ to give a second estimate of f_c. It is noted that the linear trend in the unwrapped residual phase can have either positive or negative slope, depending on whether $\hat{f}_{c,1}$ is an underestimate or an overestimate of f_c, respectively

To separate unmodulated CW from the three FMs and BPSK, use is made of the fact that the unmodulated CW carries no phase information, whereas the others do For an unmodulated CW, Tretter [12] shows that at high CNR, the complex Gaussian noise $w(n)$ has the effect of a phase noise, a real normal random variable of zero mean and variance $\sigma^2/A^2 = 1/(2\rho)$, where ρ is the CNR Since the smallest CNR considered in this study is 15dB, or 31.6, the largest phase noise variance is $1/63$ The phase noise variance is estimated by the sample average of the square of the detrended residual phase This statistic is therefore compared with the threshold of $1/50$, a value slightly larger than $1/63$. If the detrended phase statistic is smaller than this threshold, then the waveform is considered to be unmodulated CW; otherwise, the waveform is one of the three FMs or BPSK.

4. Pattern Recognition Approach

In this section, an approach based on pattern recognition techniques is proposed for discriminating between the narrow-band FM, wide-band FM, triangular FM and BPSK modulation types. The method is based on the linear discriminant technique and originally proposed in [7][8] The linear discriminant function is determined by using the sample feature vectors from the training sequence of known modulation types There are various procedures for determining the discriminant functions including statistical and non-statistical [13] In our study, the least squares approach is used for estimating the parameters of the linear discriminant functions

Let the number of classes be M; the number of feature vectors in the ith class be N_i.

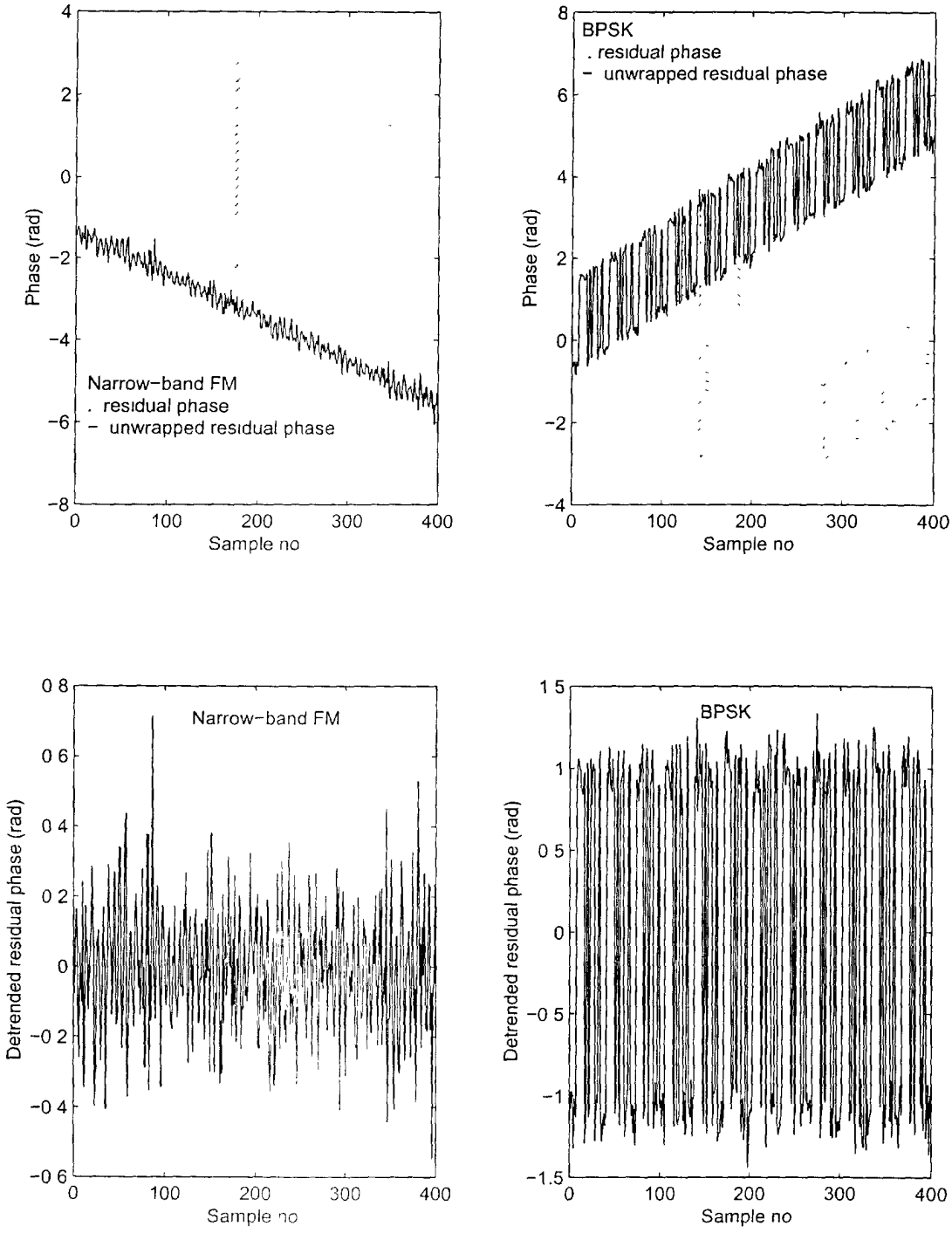

Figure 3: *Residual phase, unwrapped residual phase and detrended residual phase for narrow-band FM and BPSK modulations For narrow-band FM* $f_c = 500kHz$, $\Delta f/2 = 50kHz$, $f_m = 300kHz$ *For BPSK,* $f_c = 500kHz$, $f_{psk} = 55kHz$ $\theta = 120^{\circ}$ *Sampling frequency* $f_s = 1.8MS/s$, $N = 1024$ *and CNR=* $15dB$

The total number of feature vectors is given by $N_{total} = \sum N_i$. Denote the jth normalized feature vector of the ith class as $\underline{h}_{ij}$, and the coefficient vector of the ith class linear discriminant be $\underline{c}_i$. The normalized feature-vector matrix H is given by

$$H = [\underline{h}_{11}, \underline{h}_{12}, \ldots, \underline{h}_{MN_M}]. \tag{18}$$

Let $\underline{x}_i$ be the vector of ideal classification results of all the feature vectors by the linear discriminant of the ith class.

$$\underline{x}_i = [0, 0, \ldots, 0, \underbrace{1, 1, \ldots, 1}_{N_i}, 0, 0, \ldots, 0]^T \tag{19}$$

which is a vector of zeros except for N_i ones in the locations of the feature vectors of the ith class. The least squares approach is to minimize the following criterion with respect to $\underline{c}_i$

$$\| \underline{e}_i^T \|^2 = \| \underline{c}_i^T H - \underline{x}_i^T \|^2, \tag{20}$$

where $\|\|$ denotes the Euclidean norm. It can be verified that the minimizing solution of (20) is given by [14]

$$\underline{c}_i^T = \underline{x}_i^T H^T (H H^T)^{-1}. \tag{21}$$

In (21), the term $\underline{x}_i^T H^T$ is the sum of the transposed feature vectors of the ith class

$$\underline{x}_i^T H^T = \sum_{j=1}^{N_i} \underline{h}_{ij}^T = N_i \underline{m}_i^T, \tag{22}$$

where $\underline{m}_i$ is the mean feature vector of the ith class. The matrix HH^T is given by

$$HH^T = \sum_{i=1}^{M} \sum_{j=1}^{N_i} \underline{h}_{ij} \underline{h}_{ij}^T = N_{total} Q, \tag{23}$$

where Q is the average of $\underline{h}_{ij} \underline{h}_{ij}^T$ over all the feature vectors. Substitution of (23) and (22) into (21) gives

$$\underline{c}_i^T = \frac{N_i}{N_{total}} \underline{m}_i^T Q^{-1}. \tag{24}$$

Let $P = [\underline{c}_1, \underline{c}_2, \ldots, \underline{c}_M]^T$ Then the linear discriminant function is calculated as $P \cdot \underline{h}$, where $\underline{h}$ denotes a normalized feature vector input The output of the linear discriminant function is a vector of size M. When a feature vector is present, the decision rule of the discriminant is to assign the sequence to the class with the largest discriminant output

4.1 The Feature Vector

There is a question as to how to choose the appropriate feature vectors. In the following, we study the feature vector problem and show that there is sufficient differentiation among the detrended residual phase histograms of the three FMs and BPSK. That is, a feature vector formed from the detrended residual phase histograms shall be sufficient to discriminate between the four modulation types

In Figure 4, the results at various stages of processing that lead to the histograms for narrow-band FM are shown. The plots are numbered as increasing from left to right and from top to bottom. In plot 1, the PSD consists of a main peak and two side peaks at $\pm f_m$ from f_c, or at $200kHz$ and $800kHz$ The first estimate of the carrier frequency from the PSD, $\hat{f}_{c,1}$, is $499.90kHz$. This underestimate results in a positive slope for the unwrapped residual phase shown in plot 2. The intercept of the linear trend with the vertical axis varies from sequence to sequence because of the random initial phase ϕ in the signal model [see (4)] The detrended residual phase is shown in plot 3. Samples of the instantaneous-frequency scaled by the sampling frequency, $f(n)T$, are calculated from the detrended residual phases, $\delta\phi(n)$, according to

$$f(n)T = \frac{\delta\phi(n+1) - \delta\phi(n)}{2\pi}, \tag{25}$$

and are shown in plot 4. Although not apparent on the scale of the plots, the variations in plots 2-4 are noise-corrupted sinusoids The interval $(-\pi, \pi)$ is divided into 20 bins. The histogram of $\delta\phi(n)$ is shown in plot 5 In the absence of noise, these samples vary between $-\Delta f/2f_m$ and $\Delta f/2f_m$, or between $-1/6$ and $1/6$. Since the bin size of $\pi/10$ is greater than $1/6$, most of the samples are in the two central bins. The scaled frequency varies from -0.5 to 0.5, and this interval is also divided into 20 bins. The histogram of the scaled-frequency samples is shown in plot 6 These samples, in the absence of noise, are between $-\Delta f/2f_s$ and $-\Delta f/2f_s$, or between -0.028 and 0.028 Since the frequency histogram bin size is 0.05, most of the samples are in the two central bins.

The corresponding plots for wide-band FM are shown in Figure 5. The modulation frequency, f_m, of 400Hz is much smaller than the corresponding value of $300kHz$ in narrow-band FM The ratio $\Delta f/2f_m$ is 37.5, compared with $1/6$ for the narrow-band case Only 0.23 of a modulation cycle is sampled over the observation duration of 569 μs. There is considerable structure within the main peak of the PSD, with components at multiples of f_m on either side of f_c Since the frequency resolution, f_s/N, is

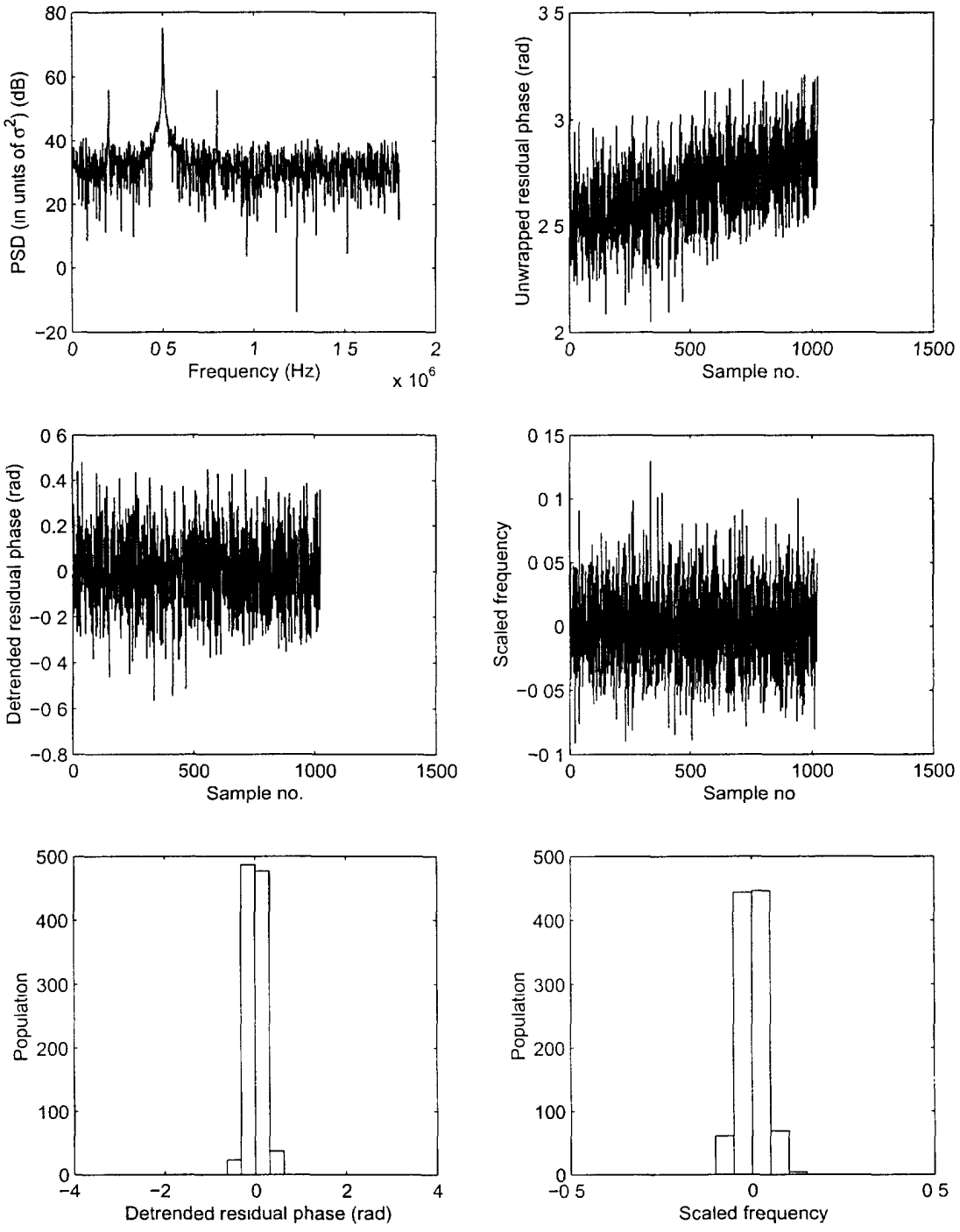

Figure 4: *The results at various stages of processing that lead to the detrended residual-phase and scaled-frequency histograms of narrow-band FM modulation The signal parameters are:* $f_c = 500kHz$, $\Delta f/2 = 50kHz$, $f_m = 300kHz$ *Sampling frequency* $f_s = 1.8MS/s$, $N = 1024$ *and CNR=* $15dB$

$1.76kHz$, this structure is not discernible. The centroid frequency is calculated to be $511.09kHz$ The unwrapped residual phase in plot 2 shows clearly that only a fraction of a modulation cycle is sampled There is no trend to speak of The fitting of a least-squares straight line, shown dashed in plot 2, is therefore not a meaningful procedure It is carried out for reason of consistency of application Due to the large value of $\Delta f/2f_m$, it is very likely that the detrended residual phase varies over a range greater than $(-\pi, \pi)$ and therefore all bins of the phase histogram are occupied. When this occurs, the first and last bins tend to be fairly highly populated, since samples smaller than $-\pi$ are placed in the first bin and samples greater than π are placed in the last bin. In the absence of noise, the scaled-frequency varies between -0.008 and 0.008. Most of the scaled-frequency samples are therefore in the two central bins, as shown in plot 6

The plots for triangular FM are shown in Figure 6. The structure within the main peak of the PSD is again not discernible The centroid frequency is $497.46kHz$ As for wide-band FM, the least-squares straight-line fit is not meaningful. Ideally, one would like to fit a line tangent to the unwrapped residual phase at the 513th sample, so that after this line is subtracted, the first 512 samples are positive and the last 512 samples are negative. As the value of the parameter Δ, which determines the slope of the instantaneous-frequency variation, increases, the detrended residual phase varies over a larger range of values, resulting in more histogram bins being occupied. However, even for the largest considered in this study, not all of the bins are occupied. For the smallest Δ values of $2kHz$ and $4kHz$, the phase histogram resembles that of narrow-band FM This is illustrated in Figure 7 for $\Delta = 2kHz$. This is the reason for the confusion between these two FMs, as will be seen from the classification results of Section 5.2.

The plots for BPSK are shown in Figure 8. The centroid frequency is $501.43kHz$. Many cycles of the bit sequence are sampled over the observation duration, and the linear trend in the unwrapped residual phase is apparent in plot 2. A least-squares straight-line fit is meaningful In the absence of noise, the detrended residual phase is either $-\theta/2$ or $\theta/2$, where $\theta = 120^o$ is the phase change when the bit state changes from zero to one It can be seen that most of the detrended residual phases are in the fourth bin on either side of zero, as shown in plot 5. There are about two samples per bit The difference between two successive detrended residual phases within the same bit is zero, is θ when there is a transition from a zero bit to a one bit, and is $-\theta$ when there is a transition from a one bit to a zero bit. As shown in plot 6, most of the scaled-frequency samples are therefore in the two central bins about zero; the scaled-frequency samples corresponding to bit-state transitions of θ and $-\theta$ are in the seventh bin on either side of zero

Figure 9 shows the case of BPSK when $\theta = 155^o$ It can be seen that the spectral value at the carrier frequency is actually lower than those of the immediate neighboring spikes, as shown in plot 1 The centroid frequency is estimated as $503.17kHz$. The behavior of the unwrapped residual phase in plot 2 seems to be related to the fact that θ is close to 180^o and to noise fluctuations. If the CNR is increased to 20dB, this

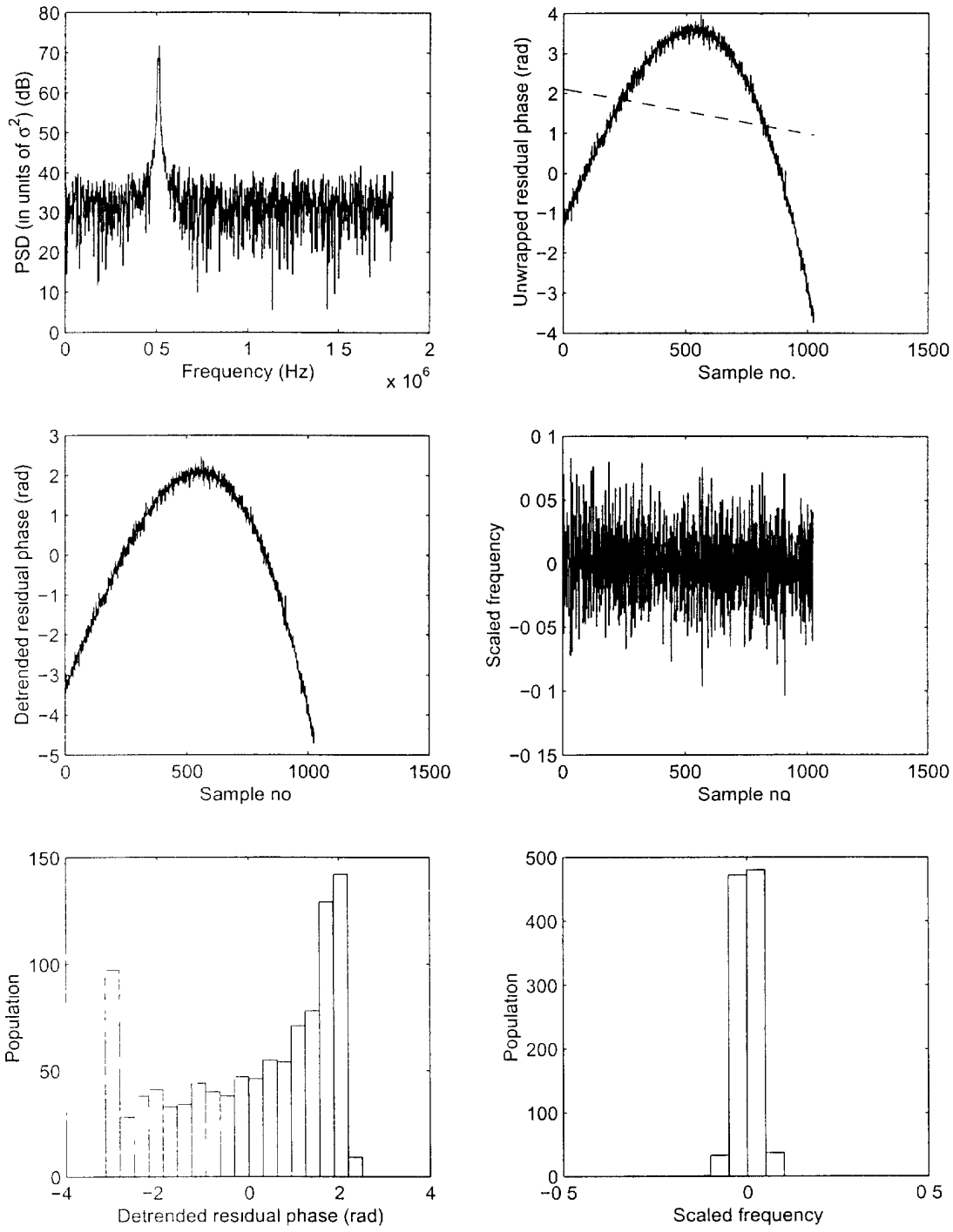

Figure 5 The results at various stages of processing that lead to the detrended residual-phase and scaled-frequency histograms of wide-band FM modulation The signal parameters are $f_c = 500kHz$ $\Delta f/2 = 15kHz$ $f_m = 400Hz$ *Sampling frequency* $f_s = 1.8MS/s$, $N = 1024$ *and CNR=* $15dB$

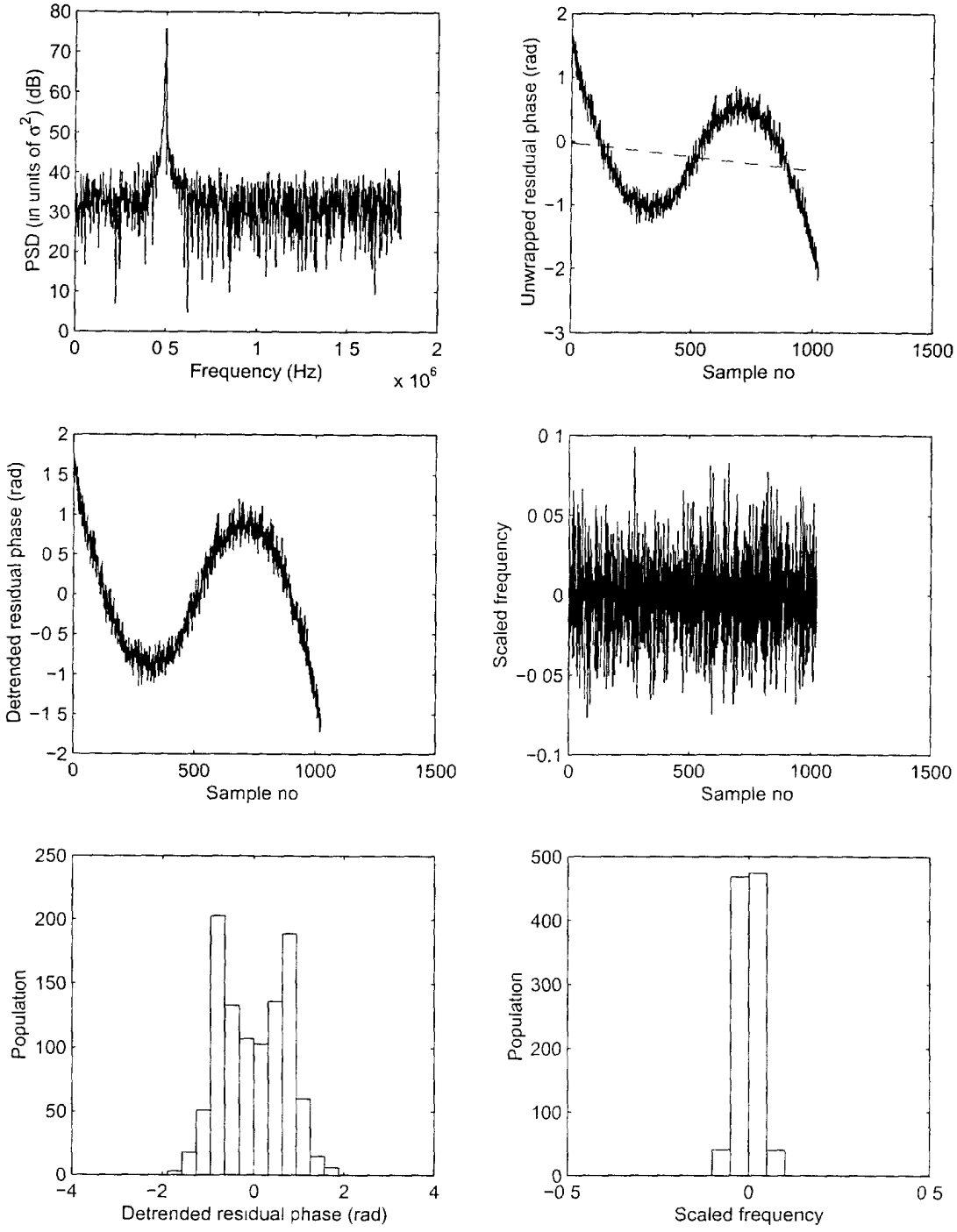

Figure 6 *The results at various stages of processing that lead to the detrended residual-phase and scaled-frequency histograms of triangular FM modulation The signal parameters are* $f_c = 500kHz$, $\Delta = 16kHz$ *Sampling frequency* $f_s = 1\,8MS/s$ $N = 1024$ *and CNR=* $15dB$

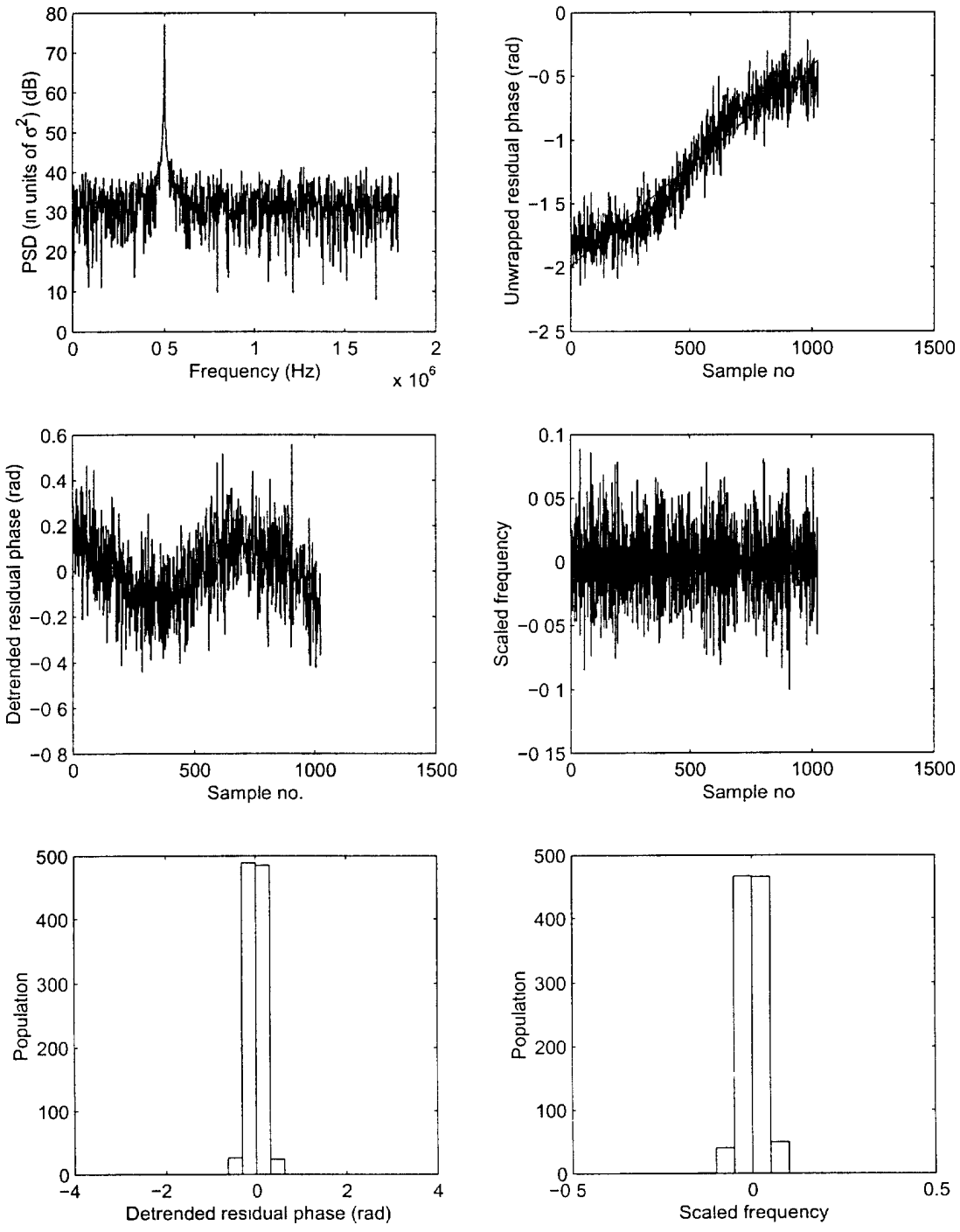

Figure 7: *The results at various stages of processing that lead to the detrended residual-phase and scaled-frequency histograms of triangular FM modulation The signal parameters are* $f_c = 500kHz$, $\Delta = 2kHz$ *Sampling frequency* $f_s = 1\ 8MS/s$, $N = 1024$ *and CNR=* $15dB$

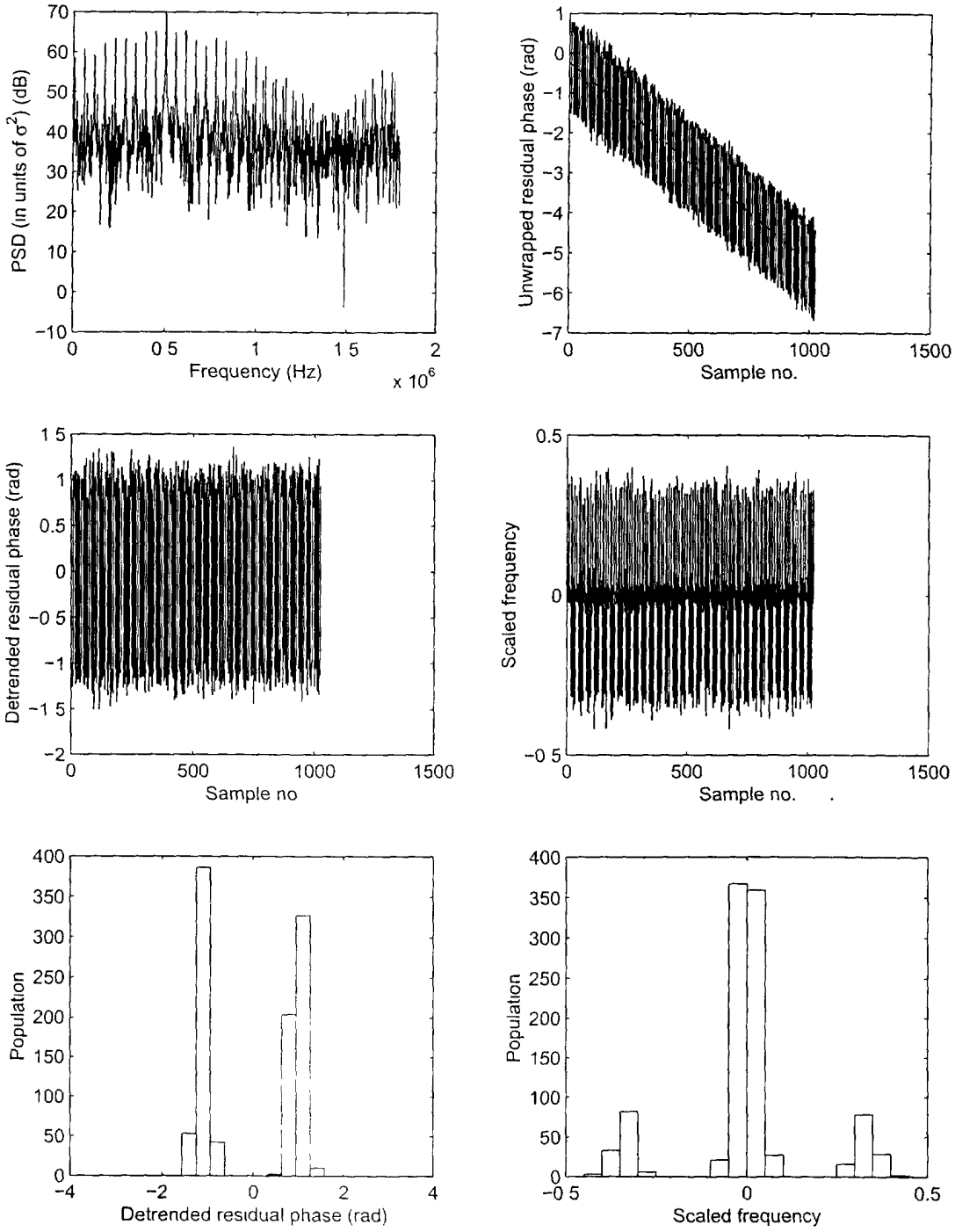

Figure 8: *The results at various stages of processing that lead to the detrended residual-phase and scaled-frequency histograms of BPSK modulation The signal parameters are: $f_c = 500kHz$, $f_{psk} = 55kHz$, $\theta = 120^o$ Sampling frequency $f_s = 1.8MS/s$, $N = 1024$ and CNR= $15dB$*

Table 1: Variation of waveform parameters for the generation of training data

Waveform	Narrow-band FM	Wide-band FM	Triangular FM	BPSK
f_c	400·100:600	400:100:600	400:100:600	500:100:700
$\Delta f/2$	40:10:60	12:3:18		
f_m	240·60:360	0.32.0 08·0.48		
Δ			2:2:18	
f_{psk}				50:5·60
θ				90, 120, 155

behavior occurs much less frequently A least squares straight-line fit to the result in plot 2 is, of course, meaningless, as is the phase histogram. This behavior results in BPSK being wrongly identified as either wide-band or triangular FM, as will be seen from the classification results of Section 5.2. The scaled-frequency histogram, however, is essentially correct, with most samples in the two central bins and those corresponding to bit-state transitions in the ninth bin on either side of zero

4.2 Training Data Generation

We have shown using numerical results that there is sufficient differentiation among the detrended residual phase histograms of the three FMs and BPSK. We use only the phase histogram as the feature vector to study the performance of the pattern recognition based approach.

Each parameter of each of the four waveforms is allowed to take on a number of values, as summarized in Table 1 In the table, the frequencies are all in kHz and the phase shifts in degrees The values are given in the form initial value:increment final value, with the exception of the phase angles of the BPSK signal. For each combination of parameter values, 20 signal sequences are simulated, varying the initial phase ϕ randomly from sequence to sequence For each signal sequence, a distinct noise sequence is generated and added to the signal sequence. The sum of the signal and noise sequences is then processed to produce the detrended residual phase histogram Since there are 27 parameter combinations and 20 sequences for each combination, 540 feature vectors are produced for each waveform. The four sets of feature vectors are concatenated in memory, giving an array The maximum population in each feature dimension, i e , in each row, is determined, resulting in a maximum-population vector p_{max} Each feature vector is normalized by p_{max}, i.e., each component of the feature vector is divided by the corresponding component of p_{max}. The result is a normalized feature-vector matrix, denoted by H.

5. Modulation Recognition Algorithm

Based on the decision theoretic and the pattern recognition approach, we propose a hybrid decision tree which is able to classify the eight modulation types efficiently In

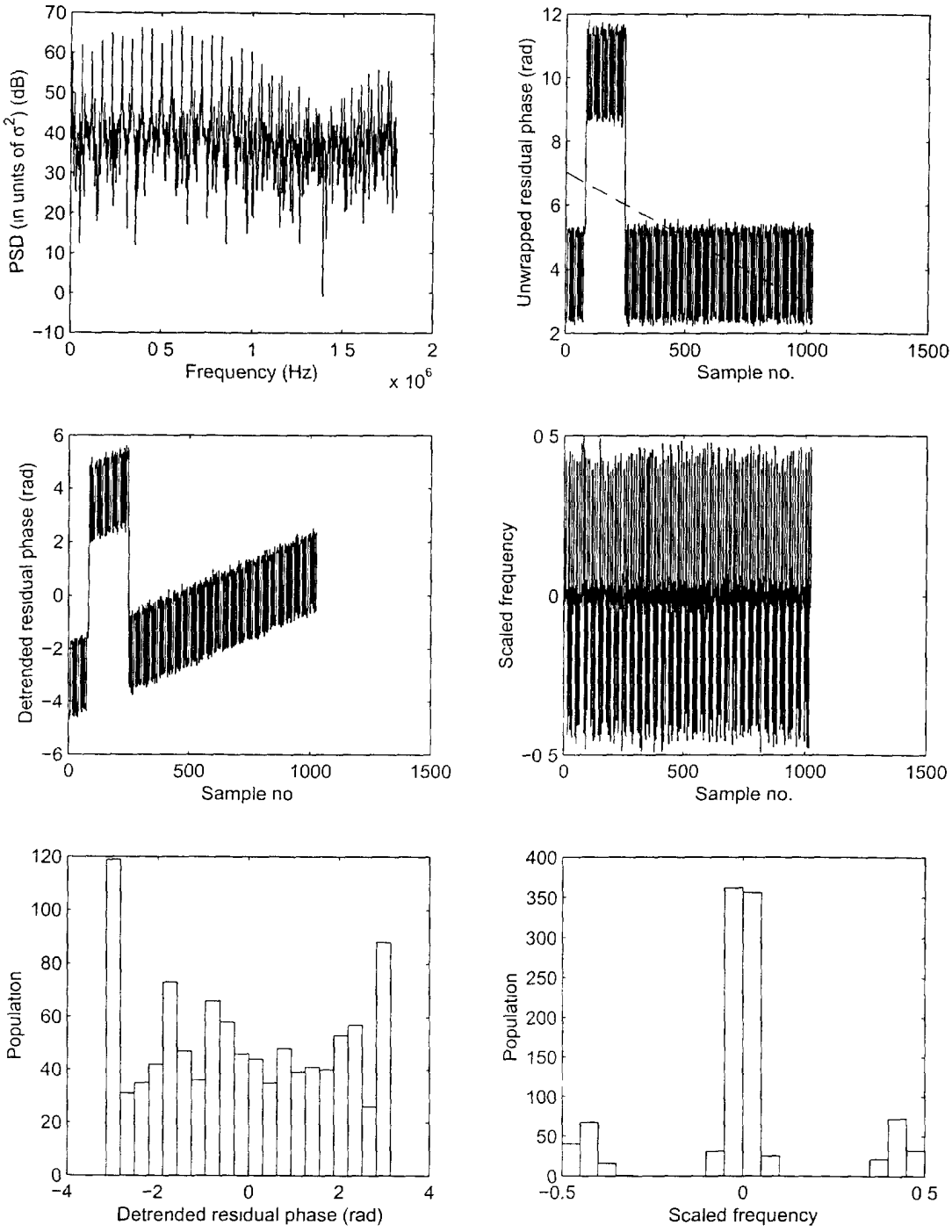

Figure 9 *The results at various stages of processing that lead to the detrended residual-phase and scaled-frequency histograms of BPSK modulation The signal parameters are* $f_c = 500kHz$, $f_{psk} = 55kHz$, $\theta = 155°$ *Sampling frequency* $f_s = 1.8MS/s$, $N = 1024$ *and CNR=* $15dB$

Table 2: Interpretation of the values of the **flag** *output of the* **modtype** *function*

Value	Modulation Type
1	Noise
2	Unmodulated CW
3	Narrow-band FM
4	Wide-band FM
5	Triangular FM
6	BPSK
7	DSB-SC
8	AM

Table 3: Contents of the output array **paramest** *of the* **modtype** *function*

Element	Parameter
1	Carrier frequency
2	Amplitude
3	FM modulation frequency
4	FM peak frequency deviation
5	Triangular FM slope
6	BPSK phase shift
7	AM modulation index
8	AM modulation frequency

the decision tree, the decision theoretic approach is used to separate noise from signals, constant-envelope waveforms from DSB-SC and AM, unmodulated CW from the three FMs and BPSK, and DSB-SC from AM while the pattern recognition approach is used to distinguish the three FMs and BPSK. The pseudocode of the decision tree for classifying the modulation type of a sample sequence is shown in Figure 10. The decision tree is implemented by the MATLAB function **modtype** The input of the algorithm is the complex sample sequence denoted by **z**. There are two outputs: **flag** and **paramest** The scalar **flag** has a value between one and eight and indicates the modulation type according to Table 2 The 1×8 array **paramest** contains the estimated values of the signal parameters The contents of **paramest** are shown in Table 3. Different subsets of the eight elements apply, depending on the waveform For the AM waveform, for example, only elements 1, 2, 7 and 8 are relevant and contain the estimated values; the other elements are zero For noise, all elements of **paramest** are zero. Values such as sampling frequency, sample size, threshold settings, etc , are required by **modtype**. These values are loaded into global memory by the script that calls **modtype** and therefore become available to it. A description of these variables is given in Table 4. In the following, we discuss in detail some of the statements in the pseudocode.

```
MODTYPE(z)
 1  Zero paramest
 2  Generate PSD
 3  Determine no  of samples, K, above TH_NOISE
 4  if K ≤ 1
 5    then flag ← 1
 6    else  Calculate PSD centroid frequency
 7          Demodulate z according to this estimate
 8          Determine envelope samples E(n) & unwrapped residual phase samples
 9            φ(n) of demodulated z
10          Calculate envelope statistic R
11          Detrend φ(n) to obtain detrended residual phase samples δφ(n)
12          if R < TH_R
13            then Calculate ⟨(δφ(n))²⟩
14                 if ⟨(δφ(n))²⟩ < TH_CW
15                   then Update f̂c
16                        Store estimates in paramest. flag ← 2
17                   else  Obtain detrended residual phase histogram
18                         Normalize histogram
19                         Calculate all linear discriminants
20                         Determine modulation type, type
21                        switch
22                          case type = narrow-band FM .
23                               Estimate fm , Δf/2 & update f̂c
24                               Store estimates in paramest. flag ← 3
25                          case type = wide-band FM :
26                               Store amplitude estimate in paramest. flag ← 4
27                          case type = triangular FM :
28                               Calculate scaled instantaneous-frequency samples f(n)T
29                               Estimate slope α & update f̂c
30                               Store estimates in paramest flag ← 5
31                          case type = BPSK :
32                               Estimate θ & update f̂c
33                               Store estimates in paramest. flag ← 6
34            else if TH_DSBSC_LOW < R < TH_DSBSC_HIGH
35                   then Estimate A , fam & fc
36                        Store estimates in paramest. flag ← 7
37                   else  Estimate m , fam & update f̂c
38                         Store estimates in paramest. flag ← 8
39  return flag, paramest
```

Figure 10 The pseudocode of the **modtype** *function*

Table 4: Values in global memory that are available to the **modtype** *function*

Variable Name	Description
fs	Sampling frequency (samples/s)
T	Sampling interval (s)
N	Sample size
n	array, containing $0, 1, \ldots, N-1$
freq_vector	array, containing $0, f_s/N, \ldots, (N-1)f_s/N$(Hz)
TH_NOISE	Threshold to separate noise from signals (volts^2)
TH_R	Threshold to separate constant-envelope waveforms from DSB-SC and AM
TH_CW	Threshold to separate unmodulated CW from the three FMs and BPSK
TH_DSBSC_LOW	Low limit of threshold range for identifying DSB-SC
TH_DSBSC_HIGH	High limit of threshold range for identifying DSB-SC
phasebc	1×20 array of detrended residual-phase histogram bin centres
range	1×20 array of largest histogram populations of the training feature vectors
dscrmnt	4×20 array of linear-discriminant coefficients

5.1 Parameter Estimation

After the modulation type is identified, the parameters of a waveform are estimated. In statements 15 and 16, the amplitude of an unmodulated CW is approximated simply by the average of the envelope samples, $< E(n) >$ The residual carrier frequency, $(f_c - \hat{f}_{c,1})$, is estimated by processing the demodulated samples $\tilde{z}(n)$ by a generalization of Crozier and collaborator's single-tone-signal-frequency estimation algorithm [9][10] This generalized algorithm is contained in the MATLAB function **dmarad** The residual-frequency estimate is then added to the first estimate based on the PSD, $\hat{f}_{c,1}$, to give the second and final frequency estimate. Alternately, **dmarad** can be applied to the input samples $z(n)$ to give the carrier-frequency estimate directly The carrier-frequency and amplitude estimates are stored in elements 1 and 2, respectively, of the **paramest** array, and **flag** is set to 2. In Figure 11, the fractional estimation error of the carrier frequency is shown in the top plot, and that of the amplitude is shown in the bottom plot The 200 sequences are the ones used to produce the classification results in Section 5 2 below The fractional estimation error is defined as (estimated value - true value)/(true value) The eight pairs of vertical lines in each plot correspond to the sequences that are misidentified as noise. In these cases, no estimates are returned and the fractional estimation errors are therefore -1 It is noted that the carrier frequency fractional estimation error is less than 10^{-4}

In statements 23 and 24, the amplitude, A, of narrow-band FM is estimated as $< E(n) >$ The slope of the least-squares straight line fit to the unwrapped residual phase is $2\pi(f_c - \hat{f}_{c,1})T$ It is therefore divided by $2\pi T$ and then added to the first estimate as given by the centroid frequency to give the carrier-frequency estimate The detrended residual phases, $\delta\phi(n)$, are expected to vary as $(\Delta f/2f_m)\sin 2\pi f_m Tn$ The **dmarad** function can be used to estimate the modulation frequency f_m. However, since the $\delta\phi(n)$ are real, whereas **dmarad** requires complex inputs, $\delta\phi(n)$ are first Hilbert

transformed The complex, transformed samples are then processed by **dmarad** to give f_m. The modulation index, $\Delta/2f_m$, is estimated by using the fact that the square of a sinusoidal signal averaged over one cycle is one-half the square of the signal amplitude Applying this to $\delta\phi(n)$, the modulation index is estimated as $\sqrt{2 < (\delta\phi(n))^2 >}$. This quantity is then multiplied by f_m to give an estimate of the peak frequency deviation, $\Delta f/2$. It is noted that this is a relatively crude way of estimating $\Delta f/2$. The detrended residual phase sequence does not, in general, contain an integral number of modulation cycles. One can use the estimate $\hat{f}_m$ to truncate the detrended residual phase sequence to an integral number of modulation cycles and calculate the mean square of the detrended residual phase based on the truncated sequence. The resulting estimate of $\Delta f/2$, however, is not much improved. Hence, at present, the entire detrended residual phase sequence is used in the estimation of $\Delta f/2$. The fractional estimation errors of the four parameters are shown in Figure 12. It is seen that the carrier and the modulation frequencies are accurately estimated, the amplitude less so, and the peak frequency deviation is least accurately estimated. The periodic nature of the peak-frequency-deviation plot is due to the loop structure used in the generation of the sample sequences. Three loops are used: the first (outermost) loop corresponds to carrier-frequency variation, the second to peak-frequency-deviation variation, and the third to modulation-frequency variation. The five cycles in the plot correspond to the five carrier-frequency values. Within each cycle, the upward-slanting lines show that the estimate becomes poorer as the modulation frequency increases, but the fact that these lines have a downward trend indicates that the estimate improves as the peak frequency deviation increases.

For wide-band FM, since a least-squares straight line fit to the unwrapped residual phase is not a meaningful procedure, none of the parameters f_c, f_m and $\Delta f/2$, is estimated In statement 26, only the coarse estimate of the amplitude is returned in **paramest**.

In statements 28, 29 and 30, the residual peak instantaneous frequency, $f_c - \hat{f}_{c,1}$, of triangular FM and the frequency slope, α, are estimated from the scaled instantaneous-frequency samples $f(n)T$. These samples can be calculated either from the detrended residual phases $\delta\phi(n)$ according to (25) or from the unwrapped residual phases $\phi(n)$ The differences between the two sets of instantaneous-frequency samples are negligible. A least-squares straight line can be fit to either the first 512 or the last 511 scaled instantaneous-frequency samples. It is found that estimates based on the last 511 samples are better The intercept of the least-squares straight line is an estimate of $(f_c - \hat{f}_{c,1})T$ It is therefore divided by T and then added to the centroid frequency to give $\hat{f}_c$. The slope of the least-squares straight line is $-\hat{\alpha}T^2$, from which $\hat{\alpha}$ is obtained. The amplitude A is estimated as $< E(n) >$.

In statements 32 and 33, only A, f_c and the phase change, θ, of BPSK are estimated. The amplitude is estimated as $< E(n) >$ The carrier frequency is estimated as in narrow-band FM The estimate of the phase change is given by

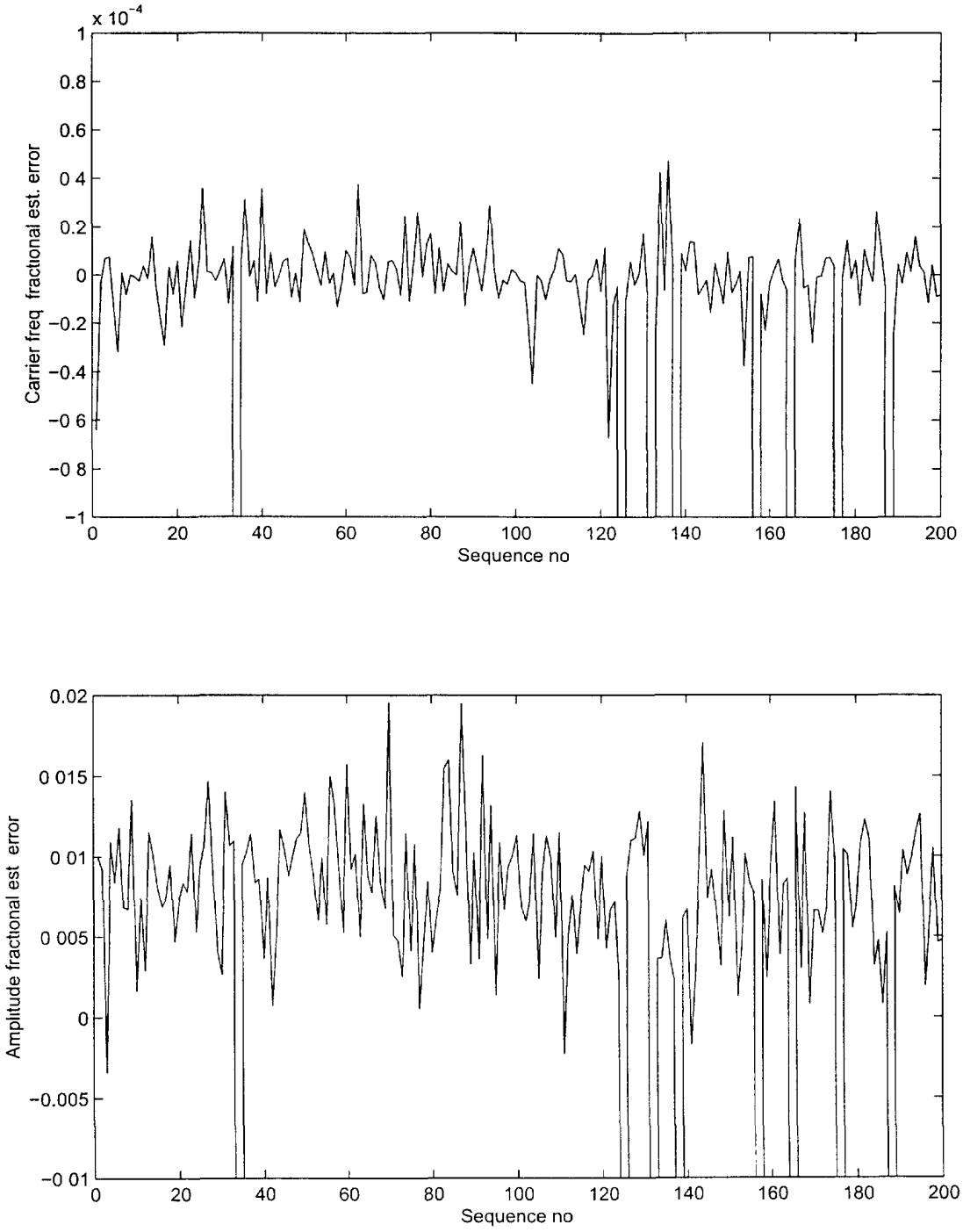

Figure 11: *Fractional estimation errors of carrier frequency and amplitude of unmodulated CW waveform Sampling frequency* $f_s = 1.8MS/s$, $N = 1024$ *and CNR=* $15dB$

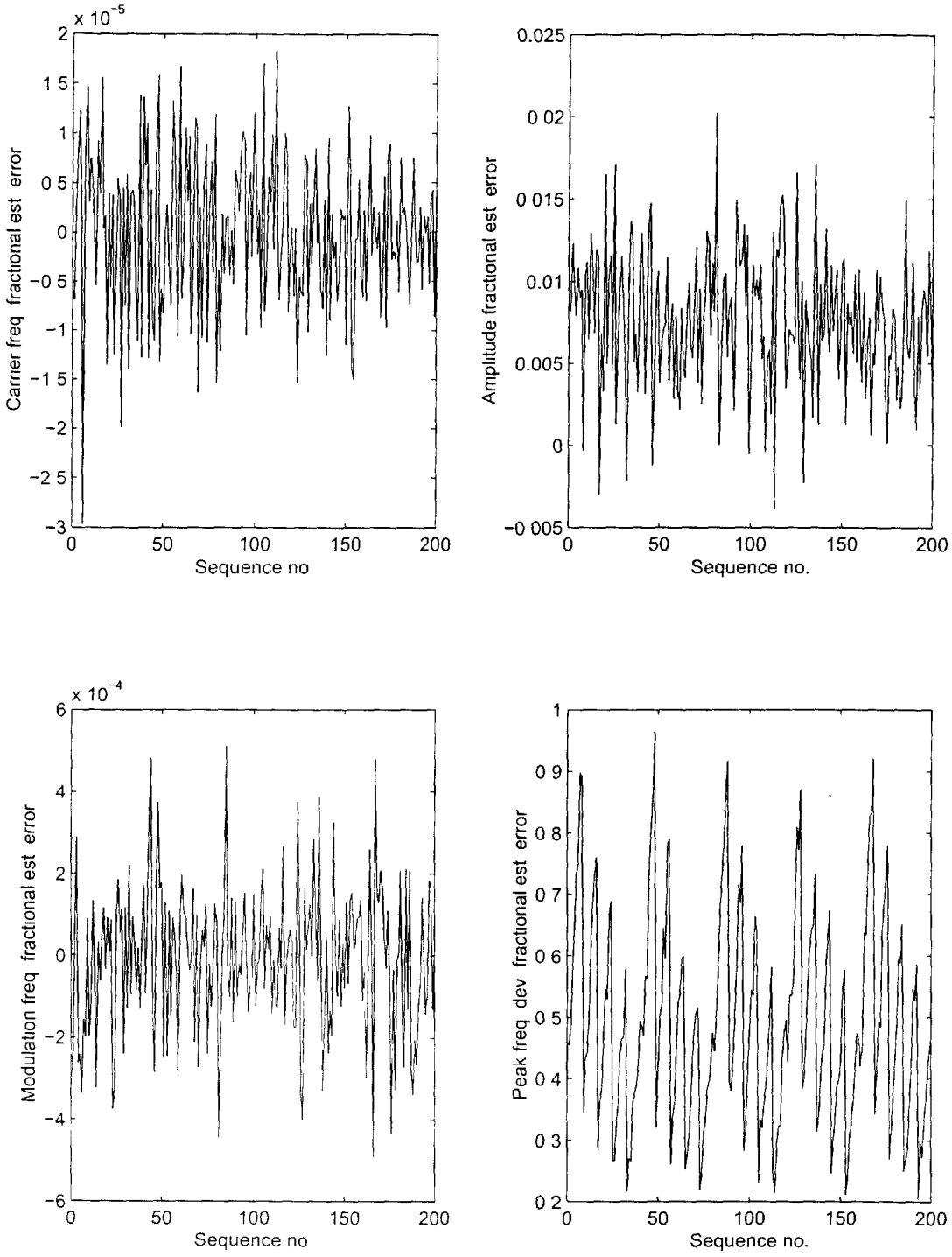

Figure 12: *Fractional estimation errors of the parameters of narrow-band FM waveform Sampling frequency* $f_s = 1.8MS/s$, $N = 1024$ *and CNR=* $15dB$

$$\hat{\theta} = 2\sqrt{< (\delta\phi(n))^2 >}. \tag{26}$$

In statements 35 and 36, the parameter A of DSB-SC cannot be estimated as $< E(n) >$ since this is approximately zero. Consider the square of the envelope. In the absence of noise, it is given by

$$E^2(n) = A^2 \cos^2(2\pi f_{am} T n) = \frac{A^2}{2}[1 + \cos(4\pi f_{am} T n)]. \tag{27}$$

From (27), we can obtain that

$$< E^2(n) >= \frac{A^2}{2}. \tag{28}$$

and

$$E^2(n) - < E^2(n) >= \frac{A^2}{2} \cos(4\pi f_{am} T n). \tag{29}$$

Thus, the amplitude A can be estimated as

$$\hat{A} = \sqrt{2 < E^2(n) >} \tag{30}$$

The carrier frequency f_{am} is estimated by the **dmarad** function. First, the Hilbert transform is applied to $E^2(n) - < E^2(n) >$ to convert them into complex values Then, the complex samples are fed to the **damard** to provide the frequency estimate f_{am} Because of the doubling of f_{am} when envelope-squared samples are considered, f_{am} should be less than $f_s/4 = 450kHz$ in order not to violate the Nyquist sampling criterion The PSD consists of two peaks, corresponding to the two sidebands; there is no peak at the carrier frequency, since it is suppressed. The carrier frequency can be estimated as in the narrow-band FM case. However, it is found that a more accurate estimate can be obtained by simply averaging the frequencies at the PSD delimiting points as given by the sample numbers n_1 and n_2. Hence, f_c is estimated as

$$\hat{f}_c = \frac{F(n_1) + F(n_2)}{2}. \tag{31}$$

where $F(n)$ are the frequency values involved in the calculation of the centroid frequency [see (14)]

For an AM signal in the absence of noise, it is noted that the normalized envelope deviation from its mean, e_n, is

$$e(n) = \frac{E(n) - < E(n) >}{< E(n) >} = m\cos(2\pi f_{am} T n), \tag{32}$$

which suggests that the modulation index, m, can be estimated as

$$\hat{m} = \sqrt{2 < e^2(n) >}. \tag{33}$$

and that the modulation frequency, f_{am}, can be estimated by the **dmarad** function after Hilbert transforming $e(n)$ The parameter A is estimated as $< E(n) >$ and the carrier frequency f_c is estimated as in narrow-band FM The fractional estimation errors of the four parameters are shown in Figure 13. Of the 200 sequences generated, 22 are misidentified as DSB-SC. The parameter estimates for the misidentified sequences are meaningless and are replaced by the true parameter values. Therefore the fractional estimation errors are zero at the misidentified sequences This can be clearly seen in plot 2, where 22 mean-envelope errors are at zero. The plots show that the modulation frequency is most accurately estimated, followed by the carrier-frequency estimate, the mean-envelope estimate, and the modulation-index estimate. The periodic nature of plot 3 is again due to the loop structure used in the generation of the sequences Three loops are involved: the first (outermost) for carrier-frequency variation, the second for modulation-frequency variation, and the third for modulation-index variation. The 25 cycles in the plot correspond to the 25 combinations of carrier frequencies and modulation frequencies. Within each cycle, the fractional error becomes smaller as the modulation index increases.

5.2 Classification Results

For each of the seven signals and noise, sequences are generated and then processed by **modtype** to evaluate its operation For noise, 10,000 sequences are generated The noise variance, σ^2, is set to unity for simplicity Each signal parameter takes on a number of values The number of sequences generated for a signal is equal to the number of parameter combinations and varies from 90 to 250 Table 5 shows the parameter values and the number of sequences generated for each signal As in Table 1, with the exception of the phase change θ of BPSK, each set of parameter values is in the form initial value:increment:final value All frequencies are in kHz, and θ is in degrees

The classification results are summarized in the confusion matrix of Table 6. The probability of false alarm is 10^{-6}, and the CNR is 15 dB. All 10,000 noise sequences are correctly identified For unmodulated CW, eight of the 200 sequences generated are misidentified as noise. This is because the randomly-chosen carrier frequency happens to be approximately equal to a multiple of the frequency resolution, f_s/N. The PSD

value at that DFT component has the value of $(AN)^2$ (78.2 dB), while the values at the other DFT components are approximately zero. Thus only one PSD value is above the noise threshold of 44.5dB, and the waveform is classified as noise.

For the triangular FM signals, of the 10 Δ values in Table 5, about 10% of the sequences are wrongly classified as narrow-band FM. The wrong classification occurs at the small $4kHz$ value of Δ. This is consistent with the discussions in Section 4.1 that for small values of the parameter Δ, the triangular FM phase histogram can be confused with that of narrow-band FM.

For BPSK, 90 sequences are generated and 64 of them are correctly identified. Of the misidentified sequences, 24 are incorrectly identified as wide-band FM and two are incorrectly identified as triangular FM. The misidentified sequences all have a phase change of $\theta = 155^o$ As discussed in Section 4.1, it is known that BPSK of a phase change of 155^o can be confused with wide-band FM or triangular FM. When classification is repeated at an increased CNR of 20 dB, the phase-unwrapping problem shown in plot 2 of Figure 9 occurs much less frequently, and all 90 sequences are correctly identified.

Of the 200 AM sequences used in the test, 178 are correctly identified. However, 22 are misidentified as DSB-SC As noted in Section 3.3, when the AM modulation index, m, is about 0.6, the square-of-envelope statistic R is approximately 0.5 and the AM waveform would be easily confused with DSB-SC. This value of m is included in the set of eight in Table 5.

6. Summary

In this report, a method for recognizing seven waveforms and noise is described. The waveforms are: unmodulated CW, narrow-band FM, wide-band FM, triangular FM, BPSK, DSB-SC and AM These waveforms are encountered in many radars of interest The method involves a combination of decision theoretic and pattern recognition techniques. The decision theoretic approach is used to separate noise from the signals, the constant-envelope waveforms from the varying-envelope waveforms, the unmodulated CW from the waveforms with phase information, and the two varying-envelope waveforms from one another The pattern recognition approach is trained to distinguish the three FM and BPSK waveforms based on their detrended residual-phase histograms. Computer simulations show that noise, narrow-band FM, wide-band FM and DSB-SC are perfectly recognized. Where confusion arises in the other four waveforms, the reasons are clearly understood Some of the confusion can be removed if some restrictions are placed on the signal parameters or by increasing the CNR.

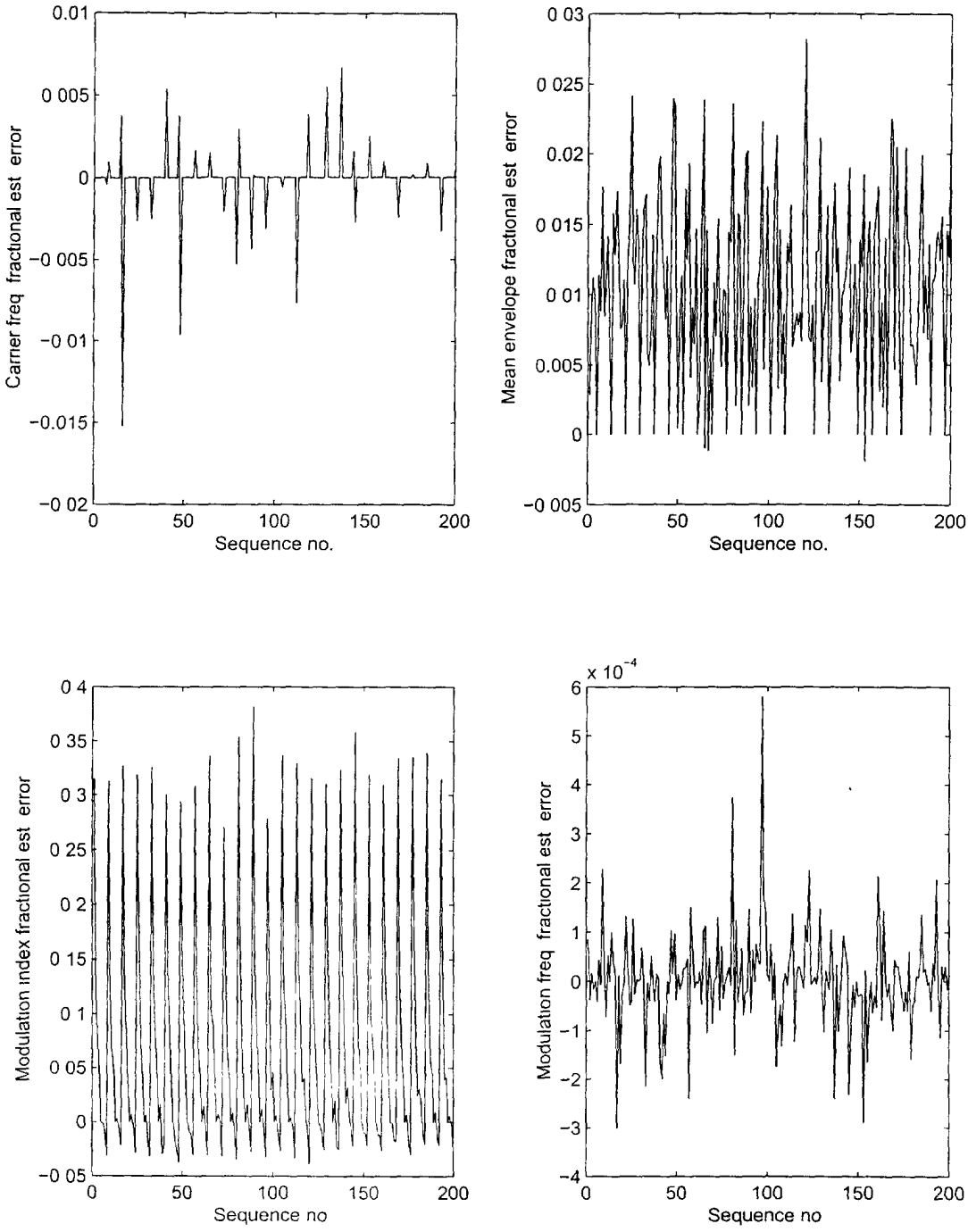

Figure 13: *Fractional estimation errors of the parameters of AM waveform Sampling frequency* $f_s = 1.8MS/s$, $N = 1024$ *and CNR=* $15dB$

Table 5: Waveform parameter values and the number of sequences generated for validation of the **modtype** *function*

Waveforms	f_c	$\Delta f/2$	f_m	Δ	f_{psk}	θ	f_{am}	m	No. Sequences
Unmodulated CW	Random from 100 to 800								200
Narrow-band FM	400:50:600	40 . 5 : 60	230 : 20 : 370						200
Wide-band FM	400:50:600	11:2:19	0 31:0 02:0 49						250
Triangular FM FM	300:50:750			4:2:22					100
BPSK	600.50 800				45.3:60	90,120,155			90
DSB-SC	350:50 800						160:10:250		100
AM	400:100:800						150 25 250	0.2 0 1:0 9	200

Table 6: *Results of waveform classification by the* **modtype** *function, CNR= 15dB*

	Noise	Unmodu-lated CW	Narrow-band FM	Wide-band FM	Triangular FM	BPSK	DSB-SC	AM
Noise	100							
Unmodulated CW	4	96						
Narrow-band FM			100					
Wide-band FM				100				
Triangular FM			10		90			
BPSK				26 7	2.2	71 1		
DSB-SC							100	
AM							11	89

References

1. E. E. Azzouz and A K. Nandi, *Automatic Modulation Recognition of Communication Signals*, Kluwer Academic Publishers, Boston, MA, 1996.

2. A. K. Nandi and E. E Azzouz, "Automatic analogue modulation recognition," *Signal Processing*, vol. 46, no. 2, pp 211-222, October 1995

3. A K. Nandi and E E Azzouz, "Algorithms for automatic modulation recognition of communication signals," *IEEE Trans. on Communications*, vol. 46, no 4, pp 431-436, April 1998

4 C. Dubuc, D. Boudreau, F. Patenaude and R. Inkol, "An automatic modulation recognition algorithm for spectrum monitoring applications," *Proc. IEEE International Conference on Communications*, Vancouver, BC., pp. 570-574, June 1999

5 Y. T Chan and L. G Gadbois, "Identification of the modulation type of a signal," *Signal Processing*, vol. 16, no 2, pp 149-154, February 1989

6 F Jondral, "Automatic classification of high frequency signals", *Signal Processing*, vol. 9, no 3, pp 177-190, October 1985

7. L. Vergara Dominquez, J. M. Paez Borrallo, J. Portillo Garcia and B Ruiz Mezcua, "A general approach to the automatic classification of radiocommunication signals," *Signal Processing*, vol. 22, no. 3, pp 239-250, March 1991

8. W S. Meisel, *Computer-Oriented Approaches to Pattern Recognition*, Academic Press, 1972.

9. S. N. Crozier and K. W. Moreland, "Performance of a simple delay-multiply-average technique for frequency estimation," *Canadian Conference on Electrical and Computer Engineering*, Toronto, Ontario, Canada, Paper WM10.3, September 13-16, 1992.

10. S. N. Crozier, "Theoretical and simulated performance for a novel frequency estimation technique," *International Mobile Satellite Conference*, Pasadena, California, pp 423-428, June 16-18, 1993

11. P. D. Welch, "The use of fast Fourier transform for the estimation of power spectra," *IEEE Trans. on Audio and Electroacoustics*, vol. AU-15, no. 2, pp. 70-73, June 1967

12. S. A. Tretter, "Estimating the frequency of a noisy sinusoid by linear regression," *IEEE Trans. on Info. Theory*, vol. 31, pp. 832-835, November 1985.

13. R. O. Duda and P. E. Hart, *Pattern Classification and Scene Analysis*, John Wiley & Sons, 1973

14. G. H. Golub and C. F. Van Loan, *Matrix Computation*, The Johns Hopkins University Press, London, 1990

Annex A
Technical and Administrative Frequency List Information

Only technical information for a station with transmit and/or receive capability is listed below Administrative information (company name, license number, etc.) is omitted.

a. station latitude

b. station longitude

c. site elevation above mean sea level (m)

d antenna height above ground (m)

e. antenna effective radiated power (dBW)

f. antenna gain (dBi)

g. antenna beam azimuth (degrees, with respect to True North)

h antenna beam polarization

This is encoded by a single upper-case letter Refer to **ant_pol.txt** to decode.

i antenna beam elevation (degrees, with respect to local horizontal)

j. antenna pattern code

This is a four-digit code. Refer to the entry with the same code in **antpat.txt** (after unzipping **antpat.zip**) for additional antenna information such as size, beam pattern, manufacturer, model number, modification date.

k. transmit and/or receive frequency (Hz)

l. bandwidth

Note the convention for specifying bandwidths: 2K06 means $2.06kHz$, 18M7 means 18 7 MHz

m. spectrum signature code

This is a three-digit code that specifies modulation type and channel capacity Refer to **sscode-e.txt**

n ITU classification of station

This is a two-upper-case-letter code. Refer to **itu_cls.txt**.

o. class of emission

This is a five-alphanumeric-character code. Only the second character is a digit; the others are letters. The first character stands for type of modulation, the second for nature of signal(s), the third for type of information, the fourth for details of signal(s), and the fifth for nature of multiplexing. Refer to **emis_cls.txt**.

p. transmitter loss (dB)

q. transmitter power (dBW)

The files **ant_pol.txt** and **itu_cls.txt** can be downloaded by going to http://apollo.ic.gc.ca/english/decode.html. The file **antpat.zip** can be downloaded and the files **sscode-e.txt** and **emis_cls.txt** can be viewed by going to http://spectrum.ic.gc.ca/tafl/tafindxe.html.

UNCLASSIFIED
SECURITY CLASSIFICATION OF FORM
(highest classification of Title, Abstract, Keywords)

DOCUMENT CONTROL DATA

(Security classification of title, body of abstract and indexing annotation must be entered when the overall document is classified)

1 ORIGINATOR (the name and address of the organization preparing the document Organizations for whom the document was prepared, e g Establishment sponsoring a contractor's report, or tasking agency, are entered in section 8)

Defence Research Establishment Ottawa

2 SECURITY CLASSIFICATION (overall security classification of the document, including special warning terms if applicable)

UNCLASSIFIED

3 TITLE (the complete document title as indicated on the title page Its classification should be indicated by the appropriate abbreviation (S,C or U) in parentheses after the title)

(U)Modulation Recognition Algorithms for Intentional Modulation on Pulse (IMOP) Applications

4 AUTHORS (Last name, first name, middle initial)

Sung Stephen and Zhou Yifeng

5 DATE OF PUBLICATION (month and year of publication of document)

December 2001

6a NO OF PAGES (total containing information Include Annexes, Appendices, etc)

38

6b NO OF REFS (total cited in document)

14

7 DESCRIPTIVE NOTES (the category of the document, e g technical report, technical note or memorandum If appropriate, enter the type of report, e g interim, progress, summary, annual or final Give the inclusive dates when a specific reporting period is covered)

DREO Technical Report

8 SPONSORING ACTIVITY (the name of the department project office or laboratory sponsoring the research and development Include the address)

DREO

9a PROJECT OR GRANT NO (if appropriate, the applicable research and development project or grant number under which the document was written Please specify whether project or grant)

1410SM 3ck11

9b CONTRACT NO (if appropriate, the applicable number under which the document was written)

W7714-990329/001/SV

10a ORIGINATOR'S DOCUMENT NUMBER (the official document number by which the document is identified by the originating activity This number must be unique to this document)

TR2001-111

10b OTHER DOCUMENT NOS (Any other numbers which may be assigned this document either by the originator or by the sponsor)

11 DOCUMENT AVAILABILITY (any limitations on further dissemination of the document, other than those imposed by security classification)

(x) Unlimited distribution
( ) Distribution limited to defence departments and defence contractors, further distribution only as approved
( ) Distribution limited to defence departments and Canadian defence contractors, further distribution only as approved
( ) Distribution limited to government departments and agencies, further distribution only as approved
( ) Distribution limited to defence departments, further distribution only as approved
( ) Other (please specify)

12 DOCUMENT ANNOUNCEMENT (any limitation to the bibliographic announcement of this document This will normally correspond to the Document Availability (11) However, where further distribution (beyond the audience specified in 11) is possible, a wider announcement audience may be selected)

Full Unlimited Anouncement

UNCLASSIFIED
SECURITY CLASSIFICATION OF FORM

DCD03 2/06/87

13 ABSTRACT (a brief and factual summary of the document It may also appear elsewhere in the body of the document itself It is highly desirable that the abstract of classified documents be unclassified Each paragraph of the abstract shall begin with an indication of the security classification of the information in the paragraph (unless the document itself is unclassified) represented as (S), (C), or (U) It is not necessary to include here abstracts in both official languages unless the text is bilingual)

In this report, the problem of signal modulation classification is investigated. A modulation recognition algorithm for classifying different signal modulation types and noise is described. The modulation type includes unmodulated CW, narrow-band FM, wide-band FM, triangular FM, BPSK, DSB-SC and AM The algorithm involves a combination of decision theoretic and pattern recognition techniques The decision theoretic technique is based on the calculation of a number of statistics of the input sequence to be classified. It is used to separate noise from the signals, the constant-envelope waveforms from the varying-envelope waveforms, the unmodulated CW from the waveforms with phase information, and the two varying-envelope waveforms from one another. The pattern recognition technique is used to distinguish the three FM and BPSK waveforms. The technique is based on the use of a linear discriminant. The discriminant is trained by feature vectors generated from the detrended residual-phase histogram Finally, computer simulations are used to demonstrate the performance of the proposed modulation recognition algorithm, and an extensive analysis is also included.

14 KEYWORDS, DESCRIPTORS or IDENTIFIERS (technically meaningful terms or short phrases that characterize a document and could be helpful in cataloguing the document They should be selected so that no security classification is required Identifiers such as equipment model designation, trade name, military project code name, geographic location may also be included If possible keywords should be selected from a published thesaurus e g Thesaurus of Engineering and Scientific Terms (TEST) and that thesaurus-identified If it is not possible to select indexing terms which are Unclassified, the classification of each should be indicated as with the title)

Modulation recognition, IMOP, radar, Decision theoretic, Pattern recognition, Linear discriminant

Defence R&D Canada
is the national authority for providing
Science and Technology (S&T) leadership
in the advancement and maintenance
of Canada's defence capabilities.

R et D pour la défense Canada
est responsable, au niveau national, pour
les sciences et la technologie (S et T)
au service de l'avancement et du maintien des
capacités de défense du Canada.

DEFENCE R&D DÉFENSE

www.drdc-rddc.dnd.ca